Journal of Paleontology, 95(3), 2021, p. 497–526

0022-3360/21/1937-2337
doi: 10.1017/jpa.2020.117

JOURNAL OF PALEONTOLOGY
A PUBLICATION OF THE Paleontological SOCIETY

Early Cambrian (Stage 4) brachiopods from the Shipai Formation in the Three Gorges area of South China

Xiaolin Duan,[1] Marissa J. Betts,[1,2] Lars E. Holmer,[1,3] Yanlong Chen,[1] Fan Liu,[1] Yue Liang,[1] and Zhifei Zhang[1]*

[1]State Key Laboratory of Continental Dynamics, Shaanxi Key Laboratory of Early Life and Environments, Department of Geology, Northwest University, Xi'an, 710069, China <duan_nwu@163.com>, <elizf@nwu.edu.cn>
[2]Division of Earth Sciences, School of Environmental and Rural Science, University of New England, Armidale, NSW 2351, Australia <marissa.betts@une.edu.au>
[3]Department of Earth Sciences, Paleobiology, Uppsala University, Villavägen 16, 752 36 Uppsala, Sweden <lars.holmer@pal.uu.se>

Abstract.—Diverse and abundant fossil taxa have been described in the lower Cambrian Shipai Formation in the Three Gorges area of Hubei Province, South China, but the taxonomy and diversity of the co-occurring brachiopod fauna are still far from clear. Here we describe the brachiopod fauna recovered from the Shipai Formation in the Three Gorges area of South China, including representatives of the subphylum Linguliformea: linguloids (*Lingulellotreta ergalievi*, *Eoobolus malongensis*, and Neobolidae gen. indet. sp. indet.), and an acrotretoid (*Linnarssonia sapushanensis*); and representatives from the subphylum Rhynchonelliformea: the calcareous-shelled Kutorginates (*Kutorgina sinensis*, *Kutorgina* sp., and *Nisusia liantuoensis*). This brachiopod assemblage and the first occurrence of *Linnarssonia sapushanensis* shell beds permit correlation of the Shipai Formation in the Three Gorges area of Hubei Province with the Stage 4 Wulongqing Formation in the Wuding area of eastern Yunnan. This correlation is further strengthened by the first appearance datum (FAD) of the rhynchonelliform brachiopod *Nisusia* in the upper silty mudstone of both the Shipai and Wulongqing formations. The new well-preserved material, derived from siliciclastic rocks, also gives critical new insights into the fine shell structure of *L. sapushanensis*. Microstructural studies on micromorphic acrotretoids (like *Linnarssonia*) have previously been restricted to fossils that were acid-etched from limestones. This is the first study to carry out detailed comparative ultrastructural studies on acrotretoid shells preserved in siliciclastic rocks. This work reveals a hollow tube and solid column microstructure in the acrotretoid shells from the Shipai Formation, which is likely to be equivalent of traditional column and central canal observed in shells dissolved from limestones.

Introduction

Brachiopods are among the most important faunal components of Palaeozoic marine communities, and have a long geological history dating back to the early Cambrian (Terreneuvian, Stage 2) (Sepkoski et al., 1981; Holmer et al., 1996; Bassett et al., 1999; Carlson, 2016; Z.F. Zhang et al., 2016; Harper et al., 2017). Many fossil brachiopods have been recovered from Cambrian Konservat-Lagerstätten (Z.F. Zhang et al., 2008, 2015; Chen et al., 2019). Of these, the Cambrian Stage 4 Shipai biota yields a diverse soft-bodied fossil assemblage, including *Vetulicola*, *Cambrorhytium*, the palaeoscolecidan *Maotianshania*, *Wronascolex*, orthothecid hyoliths (Yang and Zhang, 2016; Liu et al., 2017, 2020), and an undescribed brachiopod with tubular attachments (Zhang and Hua, 2005). Zhang et al. (2015) described a fauna of linguloid brachiopods (*Palaeobolus*, *Eoobolus*, *Lingulellotreta*) from the Shipai Formation in the Wangjiaping and Aijiahe sections, showing some general similarities in preservation with the exceptionally preserved brachiopods from the Cambrian Series 2 Chengjiang Lagerstätten. Liu et al. (2017) also documented, but did not formally describe, brachiopods from the Shipai biota in the Xiachazhuang section.

Cambrian brachiopods are widely used for biostratigraphy and correlation (Holmer et al., 1996; Skovsted and Holmer, 2005; Popov et al., 2015; Z.F. Zhang et al., 2016). Cambrian Stage 4 brachiopod assemblages had a global distribution and have been reported from Antarctica (Holmer et al., 1996; Claybourn et al., 2020), Australia (Jago et al., 2006, 2012; Smith et al., 2015; Betts et al., 2016, 2017, 2018, 2019), Greenland (Skovsted and Holmer, 2005), Siberia (Pelman, 1977; Ushatinskaya and Malakhovakaya, 2001; Ushatinskaya, 2016; Ushatinskaya and Korovnikov, 2019), the Himalaya (Popov et al., 2015), Kazakhstan (Holmer et al., 1997), and North China (Pan et al., 2019). The brachiopod assemblages previously recovered from the Cambrian Series 2 siliciclastic rocks of eastern Yunnan of China are now well known (Luo et al., 2008; Hu et al., 2013; Chen et al., 2019). Z.F. Zhang et al. (2016) documented the brachiopod assemblages from carbonate rocks of the upper

*Corresponding author

Shuijingtuo Formation in the Yangtze Platform of western Hubei Province. These faunas also permitted detailed studies of shell ultrastructure, ontogeny, and allometric development (Zhang et al., 2018a, b, 2020). However, taxonomic diversity of the brachiopod fauna from the overlying siltstones and mudstones of the Shipai Formation (Stage 4) remains unclear.

Here, we build on this earlier work by comprehensively documenting the abundant brachiopods from the silty mudstones, siltstones, and shales of the Shipai Formation in the Xiachazhuang, Wangjiaping, and Aijiahe sections, Three Gorges area, Hubei Province. The recovered brachiopod fauna comprises six families, including Acrotretidae, Lingulellotretidae, Eoobolidae, Neobolidae, Nisusiidae, and Kutorginidae. This brachiopod fauna displays close similarity to the Guanshan fauna previously described from the Wulongqing Formation (Stage 4), eastern Yunnan (Hu et al., 2013; Zhang et al., 2020a, b). Taxonomic resolution of the brachiopod fauna from the lower Cambrian Shipai Formation is an important contribution to understanding of the diversification of Cambrian brachiopods and their faunal successions in South China. It is also critical for regional biostratigraphy and correlation with other lower Cambrian terranes. Additionally, the abundant and often very well-preserved acrotretoids in the Shipai Formation display important shell structural details, providing the first opportunity to describe these structures from siliciclastics.

Geological setting

The Three Gorges area in Hubei Province of South China is located on the northern margin of the Yangtze Platform (Fig. 1.1), where Neoproterozoic and lower Paleozoic successions are well developed and widely distributed around the southeastern limb of the Huangling Anticline (Fig. 1.2). Many sections here have been suggested as standard stratigraphic sections in China (Chen et al., 2006; Wang et al., 2009), and the depositional succession along the Three Gorges area is regarded as an auxiliary stratotype section of the traditional lower Cambrian in South China (Wang et al., 1987; Zhang and Hua, 2005; Zhu et al., 2007; X.L. Zhang et al., 2008). The depositional succession through the Ediacaran–Cambrian Series 2 interval yields abundant shale-hosted fossils that have contributed significantly to the study of early animal evolution (Guo et al., 2014; Fu et al., 2019; Topper et al., 2019). The depositional sequence in the study area includes, in ascending order, the Ediacaran Dengying Formation, the lower Cambrian Yanjiahe Formation, Shuijingtuo Formation, Shipai Formation, Tianheban Formation, and Shilongdong Formation (Fig. 1.3).

The Ediacaran Dengying Formation carbonates are disconformably overlain by Terreneuvian (Fortunian–Stage 2) lower Cambrian deposits. The lowermost Cambrian unit is the Yanjiahe Formation, containing abundant small shelly fossils (SSF) that are assigned to three SSF assemblage zones (in ascending order): the *Anabarites trisulcatus-Protohertzina anabarica* assemblage zone, the *Purella antiqua* assemblage zone, and the *Aldanella yanjiaheensis* assemblage zone (Guo et al., 2008, 2014; Chang et al., 2017, 2018; Steiner et al., 2020). The Shuijingtuo Formation (black shale and limestone) disconformably overlies the Yanjiahe Formation, and has yielded abundant and diverse shelly fossils, including brachiopods, in addition to the oldest eodiscoid trilobites in South China (Wang et al., 1987; Lin et al., 2004; Steiner et al., 2007; Dai and Zhang, 2011; Yang et al., 2015; Z.F. Zhang et al., 2016; Z.L. Zhang et al., 2020). Conformably overlying the Shuijingtuo Formation is the Shipai Formation, which is dominated by yellow siltstone and grayish-yellow silty mudstone, intercalated by limestones. It is richly fossiliferous, including diverse trilobites, brachiopods, hyolithids, and bradoriids (Wang et al., 1987). The upper boundary of the Shipai Formation is marked by the contact with the argillaceous striped and oolitic limestone of the Tianheban Formation, which is itself conformably overlain by the dolomitic Shilongdong Formation (Fig. 1.3).

Materials and methods

Fossils were collected from the Shipai Formation in the Xiachazhuang, Aijiahe, and Wangjiaping sections, Three Gorges area, Hubei Province (Fig. 1). So far, >4500 individual valves have been collected from the Shipai Formation at Yichang by the work-team of the Early Life Institute (ELI), and all specimens are deposited in the Northwest University Early Life Institute, Xi'an, China. Fossils were examined under a Zeiss Smart Zoom 5 Stereo micrographic system and imaged with a Canon camera 5D Mark IV. Some specimens were analyzed with the Scanning Electron Microscope (SEM) at the State Key Laboratory of Continental Dynamics, Northwest University. When most acrotretoid specimens are cracked out, they are usually preserved as internal molds in the mudstone. In order to better display the structures, a number of latex casts were prepared with a PVB ethanol solution and latex. Some fossils and latex casts were photographed after coating with ammonium chloride (NH_4Cl).

Building on the geometric morphometric work of Zhang et al (2020a), another 16 specimens from the Shipai Formation were selected for geometric morphometric analysis (Supplementary Data 1–3). Landmarks and semi-landmarks (Fig. 9) were digitized with the free software TpsDig2 v. 2.26 (Rohlf, 2015). The data matrix was then analyzed using TpsRelw v. 1.65 (Rohlf, 2015) to explore potential changes in morphospace and to visualize shell shape using thin plate splines. The interpretation of the Cambrian Stage 4 brachiopod faunal similarities was facilitated by multivariate cluster analysis (based on Raup-Crick similarity) (Supplementary Data 4), using the computer program PAST (version 3.06; Hammer et al., 2001).

Repository and institutional abbreviation.—All fossil specimens examined in this study are housed in the following institution: The Northwest University Early Life Institute (ELI), Xi'an, China.

Systematic paleontology

Subphylum Linguliformea Williams et al., 1996
Class Lingulata Gorjansky and Popov, 1985
Order Acrotretida Kuhn, 1949
Superfamily Acrotretoidea Schuchert, 1893
Family Acrotretidae Schuchert, 1893
Genus *Linnarssonia* Walcott, 1885

https://doi.org/10.1017/jpa.2020.117 Published online by Cambridge University Press

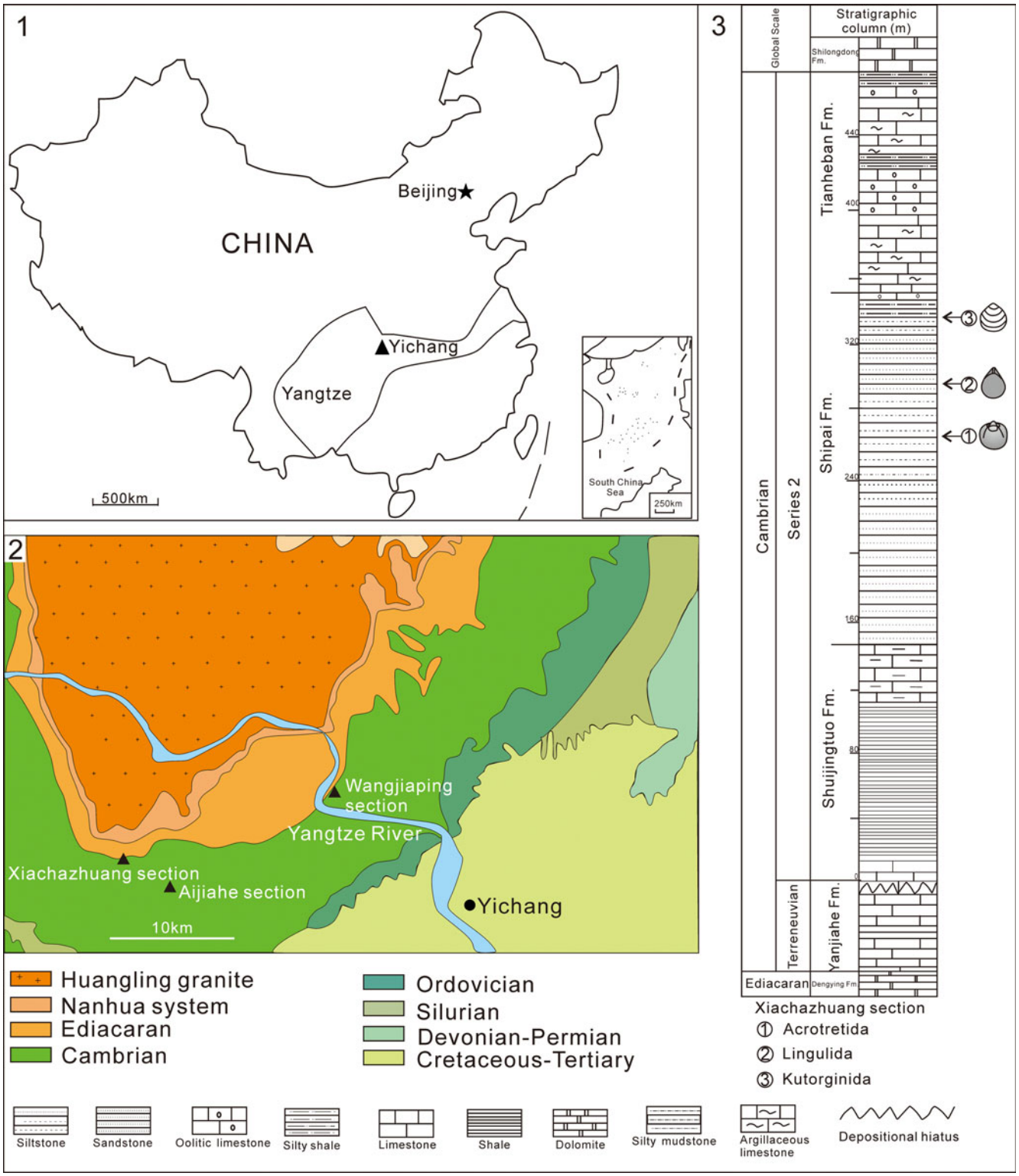

Figure 1. Simplified geological map, fossil localities, and the lithostratigraphic column of the lower Cambrian in the Three Gorges area. (**1**) Geographic map of China showing the location of Yichang. (**2**) Simplified geological map of the Three Gorges area, showing localities of the study sections. (**3**) Stratigraphic column showing the fossil horizons of brachiopods illustrated in this paper (level marked by the black arrows).

https://doi.org/10.1017/jpa.2020.117 Published online by Cambridge University Press

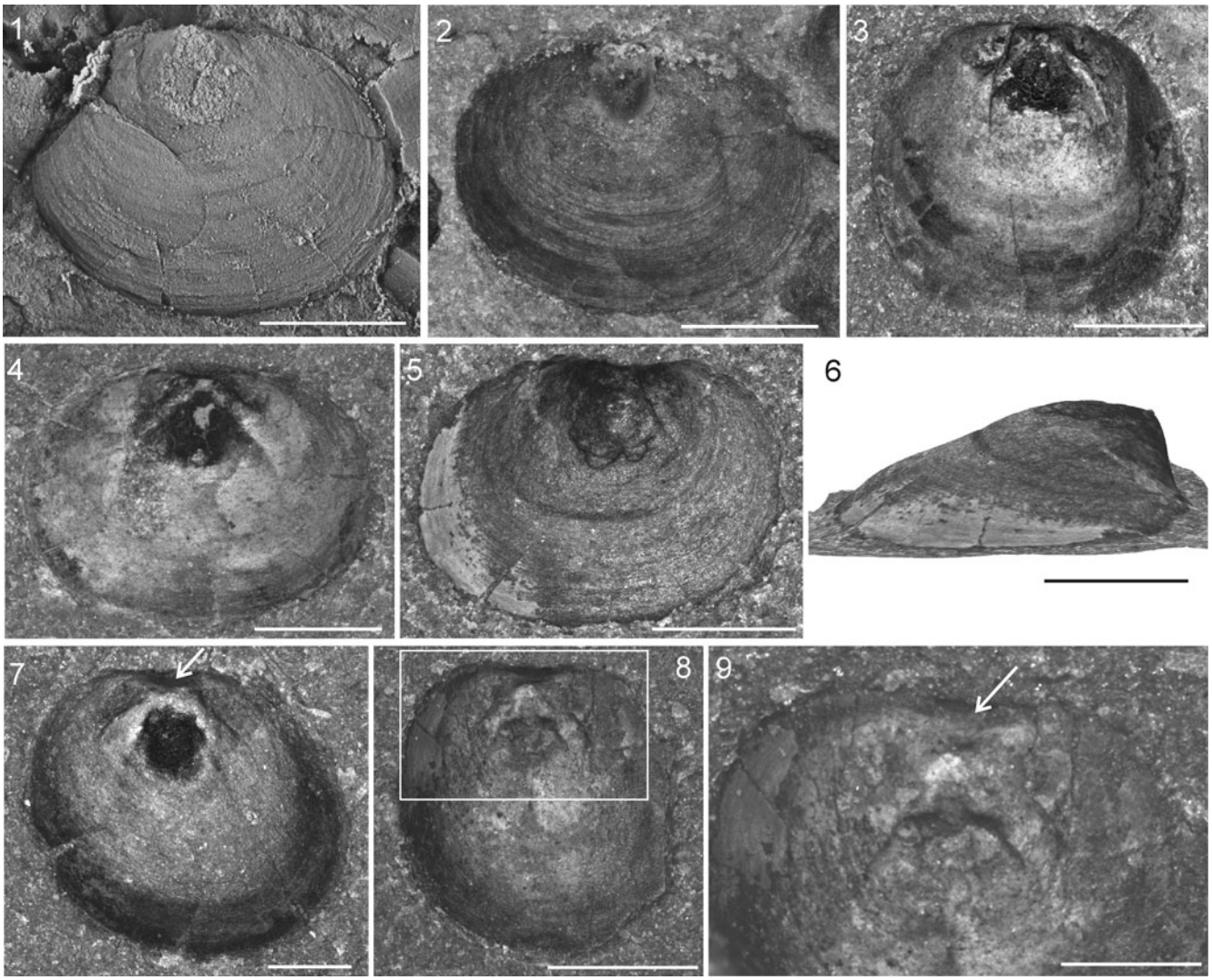

Figure 2. Ventral valves and latex cast of *Linnarssonia sapushanensis* from the lower Cambrian Shipai Formation at Xiachazhuang section. (**1**) Latex cast of ventral exterior, showing concentric growth lines on the shell surface (ELI QJP-SP-357-28); (**2**) ventral valve with concentric growth lines on the shell surface (ELI QJP-SP-289-7); (**3, 4**) internal molds (ELI QJP-SP-231, ELI QJP-SP-555-2); (**5**) internal view of ventral valve (ELI QJP-SP-041); (**6**) lateral view of (**5**); (**7–9**) internal molds showing intertrough (marked by arrows) (ELI QJP-SP-115, ELI QJP-SP-044). Scale bars = 1 mm (**1–8**), 500 μm (**9**).

Type species.—Original designation by Walcott (1885, p. 115); *Obolella transversa* Hartt in Dawson, 1868; middle Cambrian of New Brunswick, Canada.

Linnarssonia sapushanensis Duan et al., 2021
Figures 2–5, 15–17, 20

2021 *Linnarssonia sapushanensis* Duan et al., p. 41, figs. 2–4, 5.1–5.7, 6–8, 10, 11.

Holotype.—A ventral internal mold (ELI CLP-007-12) from the Wulongqing Formation (*Palaeolenus* trilobite Zone, Cambrian Stage 4) in the Sapushan section at Wuding County, eastern Yunnan Province, China (Duan et al., 2021, p. 41, fig. 2.8).

Description.—Shell ventribiconvex, subcircular to transversely oval in outline (Fig. 2). Shell valves ornamented with concentric growth lines (Fig. 2.1, 2.2).

Ventral valve convex (Fig. 2.6), with a straight to slightly convex posterior margin, lateral and anterior margins moderately rounded (Fig. 2.3–2.5); ~90% as long as wide (Table 1), with the maximum width near to mid-valve; ventral pseudointerarea varies from catacline to procline, bisected by a slightly shallow intertrough (Fig. 2.7–2.9, marked by arrows). Ventral interior (Fig. 3.1–3.11) has an apical process, characterized by a median groove that slightly expands anteriorly (Fig. 3.9, 3.10, marked by double arrows); apical process occupying ~35% of the shell length (Table 1); the vascula lateralia are impressed as pronounced ridge-like imprints. Ventral pedicle foramen continued internally forming a pedicle tube; it is preserved as a cylindrical projection with muddy infilling (Fig. 3.4, 3.5, 3.8–3.11), which is ~80 μm in diameter. Apical pits unknown. Cardinal muscle scars oval in outline (Fig. 3.9), on posterolateral slopes of valve, occupying ~22% of the shell length and ~49% of the shell width (Table 1).

Dorsal valve subcircular in outline (Fig. 4), on average 89% as long as wide (Table 1), slightly convex in lateral profile

https://doi.org/10.1017/jpa.2020.117 Published online by Cambridge University Press

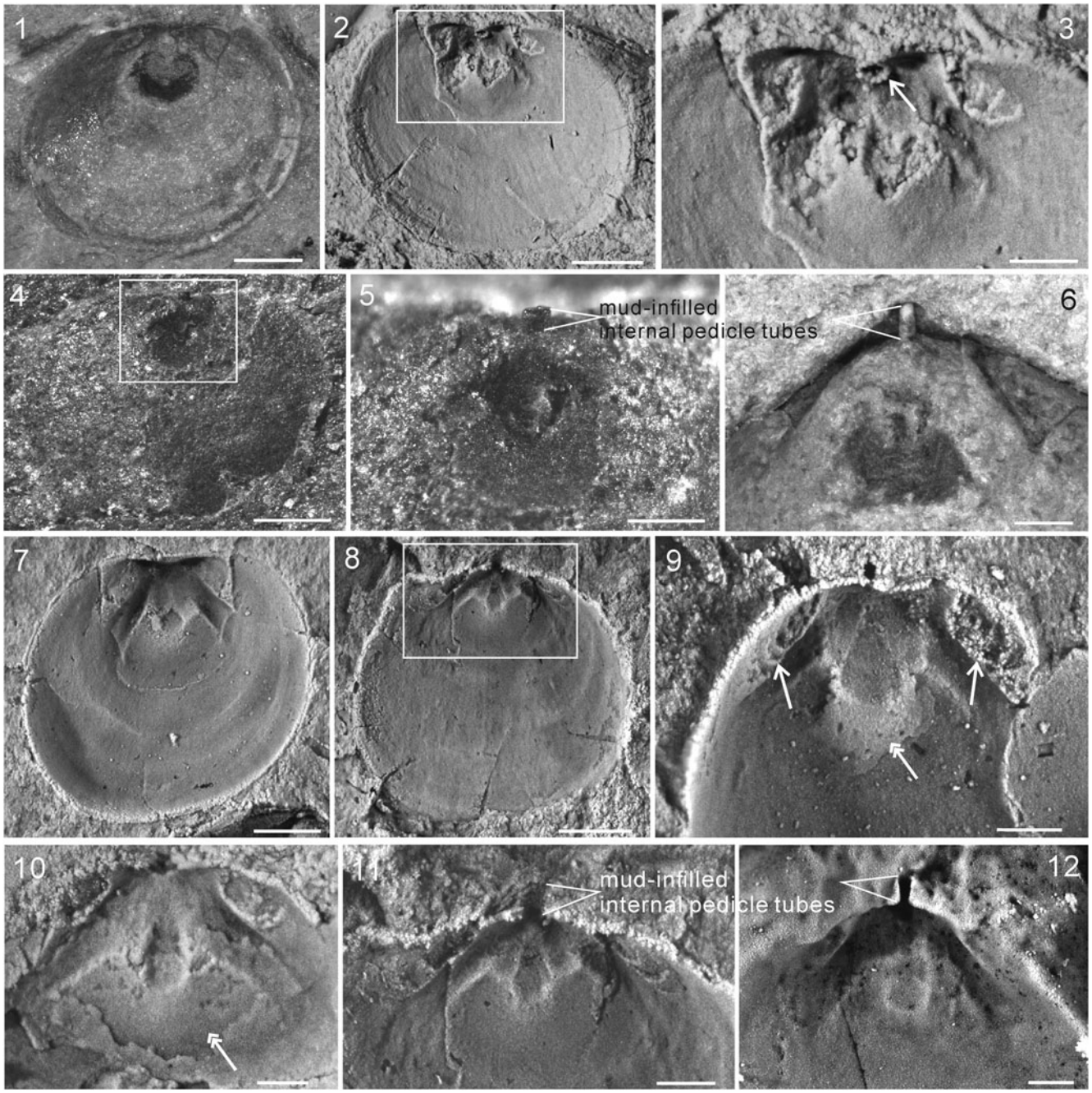

Figure 3. Ventral valves and latex casts of *Linnarssonia sapushanensis* from the lower Cambrian Shipai Formation at Xiachazhuang section, and comparison to *L. sapushanensis* from the Wulongqing Formation (Guanshan fauna). (**1**) Internal mold (ELI QJP-SP-357-2); (**2**) latex cast of (**1**); (**3**) an enlargement of (**2**), showing the pedicle opening (marked by arrow); (**4**) internal mold (ELI QJP-SP-040); (**5**) close-up view of (**4**), note the mud-infilled internal pedicle tube; (**6**) one specimen of *L. sapushanensis* with the mud-infilled pedicle tube from the Wulongqing Formation, eastern Yunnan (ELI CLP-007-12); (**7, 8**) latex casts (ELI QJP-SP-357-30, ELI QJP-SP-357-30); (**9**) latex cast showing cardinal muscle scars (marked by arrows) and apical process with a median groove (marked by double arrows) (ELI QJP-SP-357-37); (**10**) latex cast showing apical process with a median groove (marked by double arrows) (ELI QJP-SP-357-9); (**11**) an enlargement of (**8**), note the latex cast of mud-infilled internal pedicle tube; (**12**) latex cast of *L. sapushanensis* from the Wulongqing Formation, eastern Yunnan (ELI CLP-183-30). Scale bars = 500 μm (**1, 2, 4, 7, 8**), or 200 μm (**3, 5, 6, 9–12**).

(Fig. 4.4), with the maximum height near to the posterior one-fourth of shell length; dorsal pseudointerarea small and orthocline, characterized by a small rudimentary proparea and transversely elongate, subtriangular median groove. Dorsal valve interior with prominent median buttress; dorsal median septum well developed, starting directly anterior of median buttress and extends ~60% of the valve length, the terminal portion of the median septum forms a triangular platform-like swelling (Fig. 4.1–4.3, 4.7–4.10). Cardinal muscle scars are prominent and widely separated (Fig. 4.5), extending anterolaterally from the lateral edge of the median groove, occupying ~25% of the shell length and ~48% of the shell width (Table 1).

https://doi.org/10.1017/jpa.2020.117 Published online by Cambridge University Press

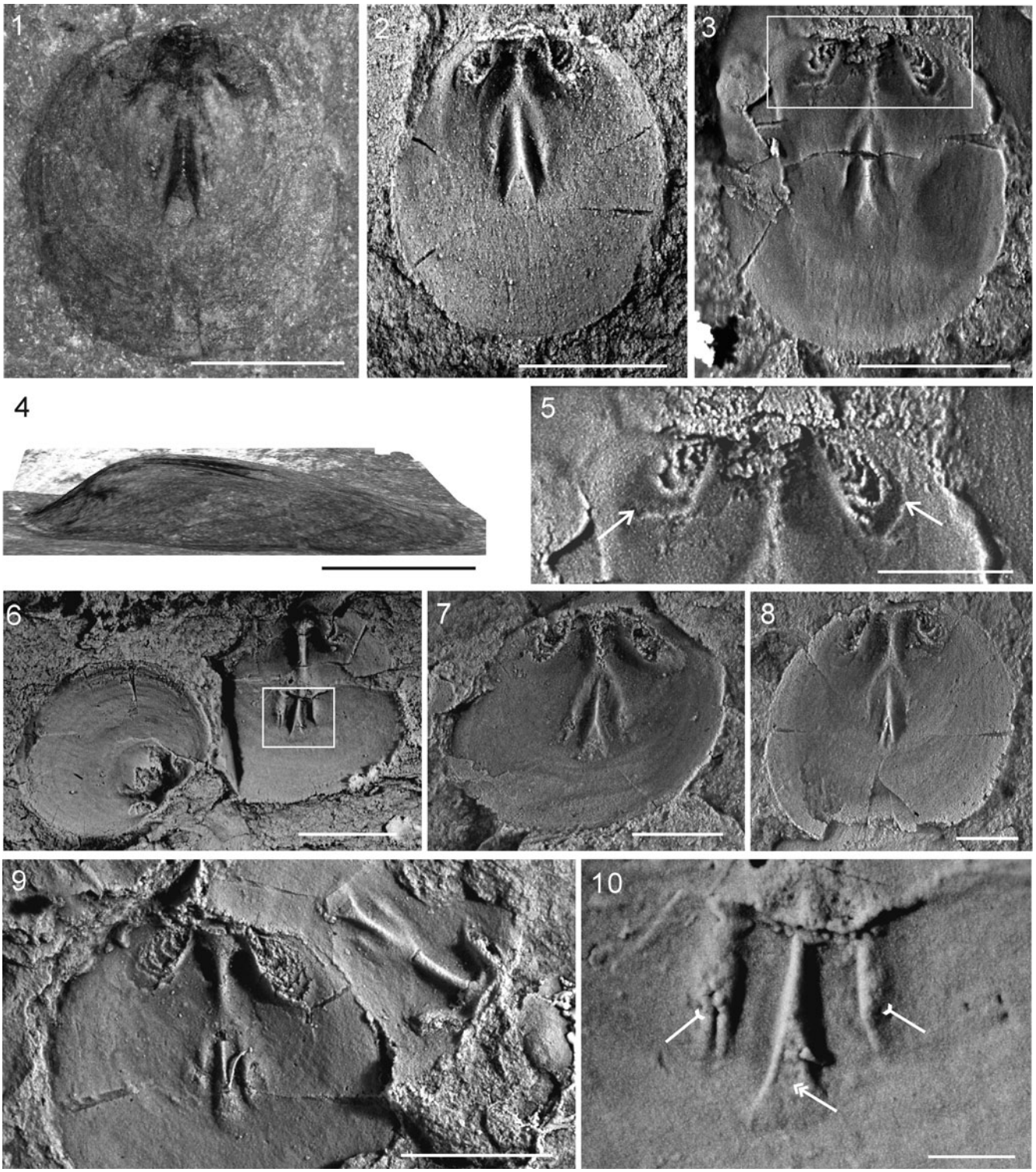

Figure 4. Dorsal valves and some relative latex casts of *Linnarssonia sapushanensis* from the lower Cambrian Shipai Formation at Xiachazhuang section. (**1**) Internal mold (ELI QJP-SP-120); (**2**) latex cast of (**1**); (**3**) latex cast (ELI QJP-SP-357-25); (**4**) lateral view of (**1**); (**5**) enlargement of (**3**), showing the cardinal muscle scars (marked by arrows); (**6–9**) latex casts (ELI QJP-SP-357-1, ELI QJP-SP-357-23, ELI QJP-SP-357-24, ELI QJP-SP-357-38); (**10**) close-up view of (**6**), showing the anterocentral muscle scars (marked by tailed arrows) and subtriangular platform-like swelling of the terminal portion of median septum (marked by double arrows). Scale bars = 1 mm (**1–4, 6, 9**), 500 μm (**5, 8**), or 200 μm (**7, 10**).

https://doi.org/10.1017/jpa.2020.117 Published online by Cambridge University Press

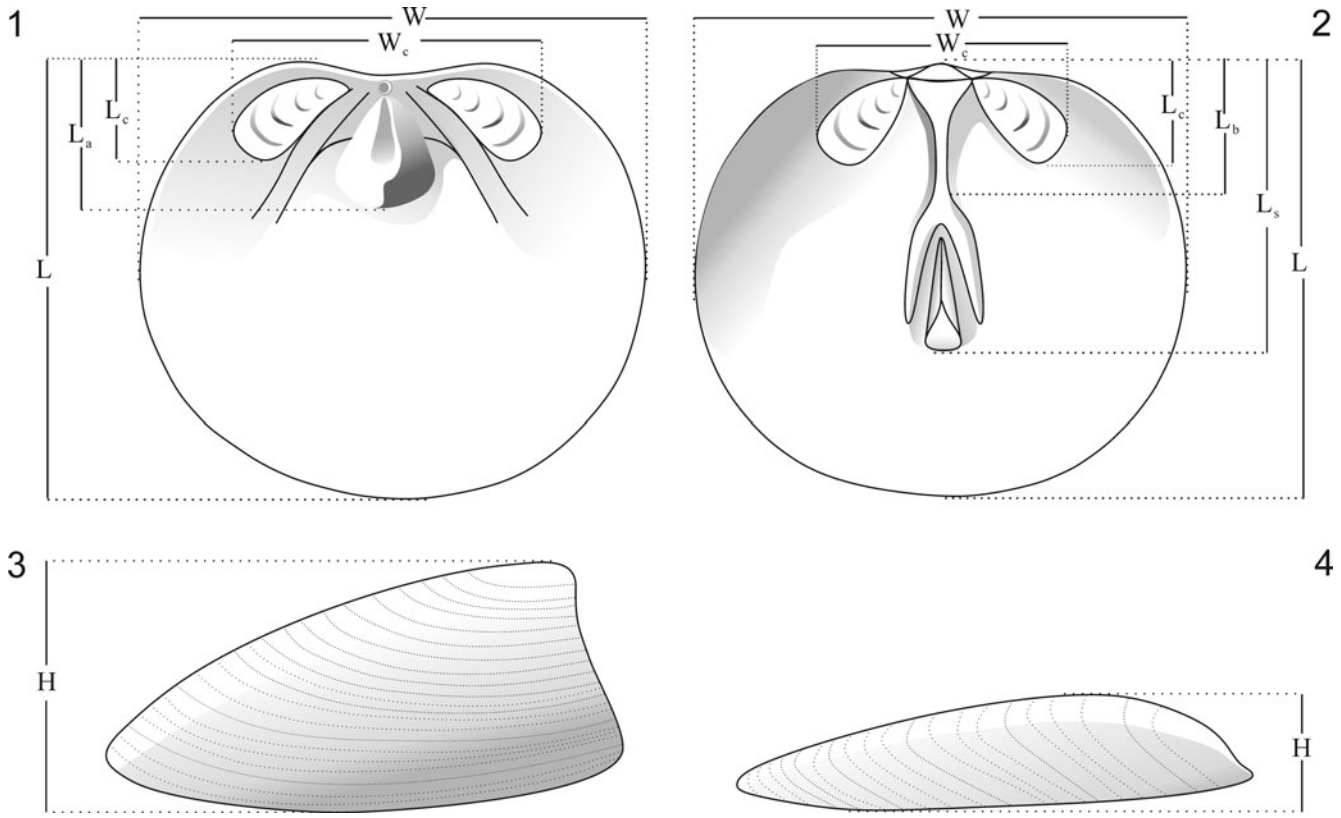

Figure 5. Schematic reconstruction of *Linnarssonia sapushanensis* from lower Cambrian Shipai Formation, showing location of measurements in Table 1. (**1**) Ventral interior; (**2**) dorsal interior; (**3**) lateral view of ventral valve; (**4**) lateral view of dorsal valve.

Materials.—ELI QJP-SP-001-613, ELI AJH-SP-001-136. There are 749 slabs collected from the middle to upper part of the Shipai Formation in the Xiachazhuang and Aijiahe sections. However, the exact number of individual ventral and dorsal valves can only be approximated because many specimens overlap each other. As of now, 484 specimens have been examined and photographed.

Remarks.—In the Shipai Formation, acrotretoid brachiopod shells are preserved as patchy aggregations on the bedding plane, while acrotretoids from the Wulongqing Formation form thicker shell beds (~11–13 pavements within 1 cm thick bed). Morphology of the specimens from the Shipai Formation is similar to *L. sapushanensis* Duan et al., 2021 from the lower Cambrian Wulongqing Formation (Stage 4). Both taxa have a similar shell outline, catacline to procline ventral pseudointerarea, a pronounced dorsal median buttress, and cardinal muscle scars, as well as similar dimensions and ratios of key characters of the ventral valves (*L. sapushanensis* from the Wulongqing Formation: L/W = 89%, L_a/L = 34%, L_c/L = 21%; Duan et al., 2021; data of the specimens from the Shipai Formation in Table 1, and location of measurements in Fig. 5).

Order Lingulida Waagen, 1885
Superfamily Linguloidea Menke, 1828
Family Lingulellotretidae Koneva and Popov, 1983
Genus *Lingulellotreta* Koneva and Popov, 1983

Type species.—*Lingulellotreta ergalievi* Koneva in Gorjansky and Koneva, 1983, early Cambrian (Stage 4) Shabakty Group, Malyi Karatau, Kazakhstan.

Lingulellotreta ergalievi Koneva in Gorjansky and Koneva, 1983
Figure 6

1983 *Lingulellotreta ergalievi* Koneva in Gorjansky and Koneva, p. 132, figs. 1–8.
1997 *Lingulellotreta malongensis*; Holmer et al., p. 581, fig. 4.1–4.14.
2004 *Lingulellotreta malongensis*; Li and Holmer, p. 193, fig. 9.
2016 *Lingulellotreta malongensis*; Z.F. Zhang et al., p. 347, fig. 10F.

Holotype.—A ventral valve interior, MIGSA (Museum of Geology, Institute of Geological Sciences, Almaty, Kazakhstan) from the early Cambrian (Stage 4) Shabakty Group, Malyi Karatau, Kazakhstan (Gorjansky and Koneva, 1983, p. 132, pl. 28, fig. 1).

Description.—Shell tear-shaped in outline (Fig. 6), ~142% as long as wide with maximum width anterior to mid-length; ventral valve length 4.50 mm and width 3.37 mm on average; ventral pseudointerarea orthocline and triangular (Fig. 6.4, 6.5), with well-developed flexure lines, occupying 75% of

https://doi.org/10.1017/jpa.2020.117 Published online by Cambridge University Press

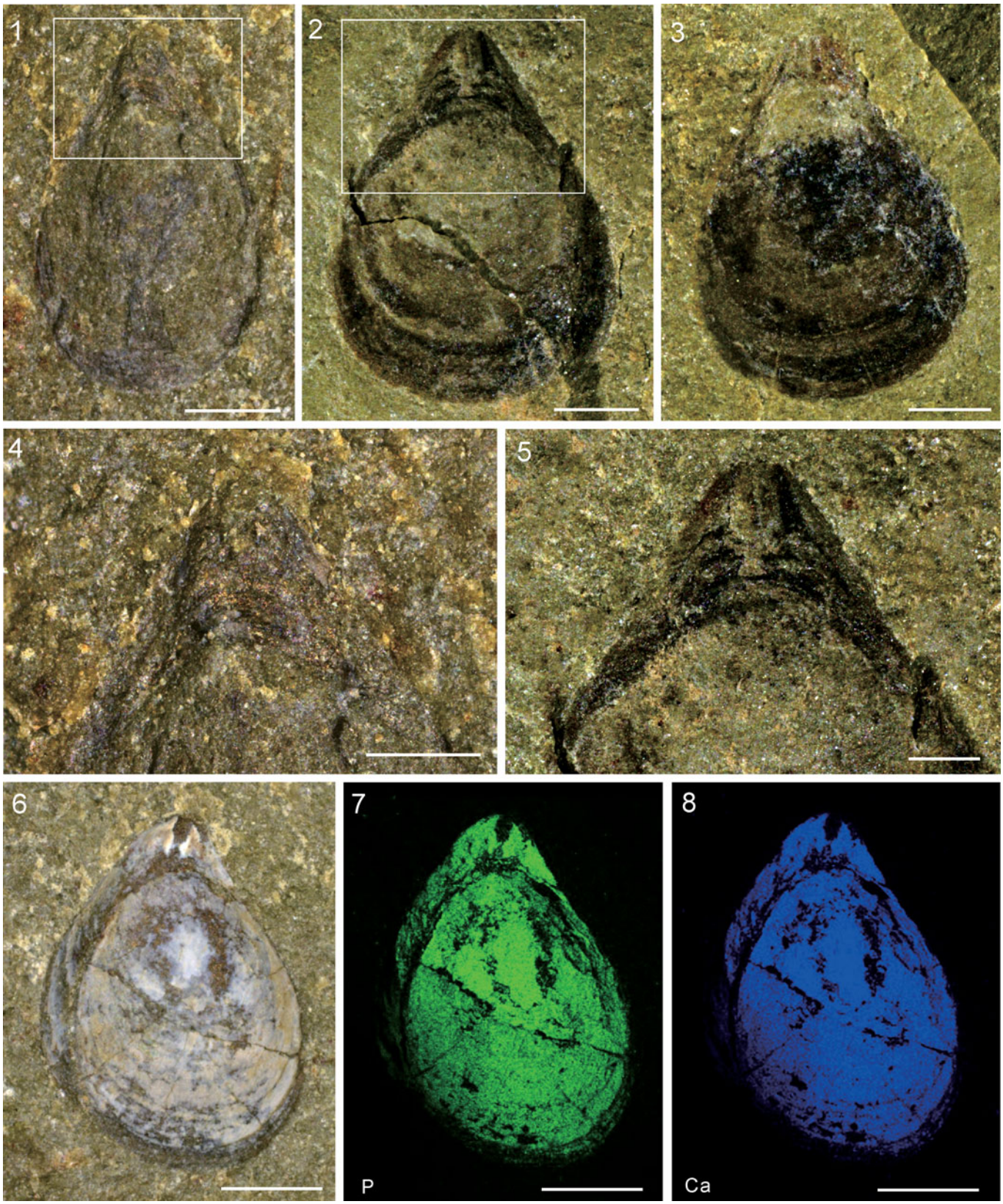

Figure 6. The linguloid *Lingulellotreta ergalievi* from the lower Cambrian Shipai Formation at Xiachazhuang and Wangjiaping sections. (**1**) Ventral valve (Xiachazhuang section) (ELI QJP-SP-173); (**2, 3**) ventral valves (Wangjiaping section, from Zhang et al., 2015) (ELI SPB-L002A, ELI SPB-L002B); (**4**) close-up view of (**1**) showing pseudointerarea; (**5**) enlargement of (**2**), showing the elongate oval foramen and well-developed pseudointerarea; (**6**) ventral valve (ELI QJP-SP-039); (**7, 8**) Elemental maps of (**6**) using micro X-ray fluorescence, showing the rich concentration of Ca and P on the conjoined shell valves. Scale bars = 1 mm (**1–3, 6–8**), or 500 μm (**4, 5**).

https://doi.org/10.1017/jpa.2020.117 Published online by Cambridge University Press

valve width and 37% of valve length; elongate oval pedicle foramen placed at posterior tip of pseudointerarea with average apical angle of 69°; foramen 0.22 mm wide on average, occupying 31% of the length and 9% of the width of the pseudointerareas; pedicle foramen usually preserved as a mud-infilled ridge or groove.

Shell surface bears weakly developed concentric growth lines. Shell shows a strong elemental abundance of Ca and P, compared with the surrounding rock in the μ-XRF study (Fig. 6.7, 6.8), suggesting that the original composition of the shell is calcium phosphate.

Materials.—Eleven specimens (including fragments) collected from middle-upper part of the Shipai Formation at the Xiachazhuang and Wangjiaping sections.

Remarks.—The first record of *Lingulellotreta ergalievi* Koneva in Gorjansky and Koneva, 1983 was from the lower Cambrian Shabakty Group (*Ushbaspis limbata* Zone) of the Malyi Karatau Range, south Kazakhstan (Gorjansky and Koneva, 1983). Holmer et al. (1997) restudied the material and made detailed morphological comparison to specimens described as "*L.*" *malongensis* (Rong, 1974) by Jin et al. (1993) from the Chengjiang fauna in eastern Yunnan, and argued that "*L.*" *malongensis* from the Chengjiang fauna should be referred to *Lingulellotreta*, and therefore that *L. malongensis* be regarded as a senior synonym of *L. ergalievi*. Zhang et al. (2020a) compared brachiopods from the Chengjiang and Guanshan faunas, and referred the species in the Chengjiang Lagerstätte to *Lingulellotreta yuanshanensis* Zhang et al., 2020a and the species from the Guanshan Biota to *Eoobolus malongensis* (Rong, 1974). Zhang et al. (2020a) demonstrated that *L. yuanshanensis* from South China (Chengjiang fauna) differs from the Kazakhstan *Lingulellotreta ergalievi* in several characters, including the ratio of valve length and width, the apical angle, and the longer ventral pseudointerarea ($L_p/L = 49\%$ in *L. yuanshanensis* from Chengjiang fauna, South China; $L_p/L = 34\%$ in *L. ergalievi* from South Kazakhstan) (see measurements in Zhang et al., 2020a).

However, specimens from the Shipai Formation described herein have striking similarities to *L. ergalievi* from the lower Cambrian Shabakty Group, Malyi Karatau Range of South Kazakhstan (Holmer et al., 1997). These include an orthocline ventral valve pseudointerarea, as well as similar outlines and similarities in the ratios of the ventral valve (herein: $L/W = 142\%$, $L_p/L = 37\%$; Holmer et al., 1997: $L/W = 139\%$, $L_p/L = 34\%$ of ventral valves). Thus, the formerly so-called *L. malongensis* from the Shipai Formation at the Wangjiaping section (Zhang et al., 2015) should be referred to *L. ergalievi*.

Family Eoobolidae Holmer, Popov, and Wrona, 1996
Genus *Eoobolus* Matthew, 1902

Type species.—*Obolus* (*Eoobolus*) *triparilis* Matthew, 1902; middle Cambrian (Amgian, Bourinot Group), Cape Breton, Canada.

Eoobolus malongensis Rong, 1974
Figures 7–10

1974 *Lingulepis malongensis* Rong, p. 114, pl. 44, figs. 27, 32.
non 1993 *Lingulepis malongensis* (Rong); Jin et al., p. 794, figs. 5.1, 5.6, 5.7, 8.1–8.4, 9.4.
non 1997 *Lingulellotreta malongensis* (Rong); Holmer et al., p. 581, fig, 4.1–4.14.
non 2000 *Lingulellotreta malongensis* (Rong); Holmer and Popov, p. H72, fig. 34, 1a–d.
non 2004 *Lingulellotreta malongensis* (Rong); Zhang et al., p. 4, figs. 1, 2.
non 2004 *Lingulellotreta malongensis* (Rong); Hou et al., p. 182, fig. 17.3.
?2004 *Eoobolus* aff. *viridis* (Cobbold, 1921); Li and Holmer; p. 197, figs. 6, 7.
non 2004 *Lingulellotreta malongensis* (Rong); Li and Holmer, p. 199, fig. 9.
non 2005 *Lingulellotreta malongensis* (Rong); Zhang et al., p. 279, figs. 1f–h, 2f, g, i, j, 3b–j.
non 2007a *Lingulellotreta malongensis* (Rong); Zhang et al., p. 65, figs. 1–3.
non 2008 *Lingulellotreta malongensis* (Rong); Z.F. Zhang et al., p. 243, figs. 4k–n, 6a.
non 2012 *Lingulellotreta malongensis* (Rong); Liu et al., p. 127, fig. 2g.
non 2013 *Lingulellotreta malongensis* (Rong); Hu et al., p. 146, fig. 193.
?2015 *Eoobolus* sp.; Zhang et al., p. 175, fig. 6.
?2016 *Eoobolus* aff. *viridis* (Cobbold, 1921); Z.F. Zhang et al., p. 347, fig. 10a–e.
2020a *Eoobolus malongensis* (Rong); Zhang et al., p. 21, figs. 2–4.

Neotype.—The holotype is unfortunately lost, but was formerly housed in the Nanjing Institute of Geology and Palaeontology (NIGP 22154). Recently, a neotype was selected (ELI-CLP 012) from the Wulongqing Formation, Malong County, eastern Yunnan Province, China (Zhang et al., 2020a, p. 4, fig. 2A, B).

Description.—Shell ventro-biconvex, tear-shaped to elongate sub-triangular in outline (Figs. 7, 8), Shell valves ornamented with concentric growth lines (Fig. 7.2). Ventral valve acuminate (Fig. 7.2–7.6), with apical angle ~78° on average; ventral valve length 3.23 mm and width 2.45 mm on average (Table 3), with the maximum width anterior to mid-valve; ventral pseudointerarea triangular, close to orthocline, occupying 37% of valve length and 75% of valve width. Pedicle groove deep with parallel lateral margins, infilled and preserved as parallel-sided ridge; ~0.7 mm in length and ~0.2 mm in width, and extending anteriorly to ~20% of total valve length. Ventral visceral area with a 'U'-shaped impression of pedicle nerve extending to one-third valve length (Fig. 7.7, 7.8).

Dorsal valve sub-oval in outline (Fig. 8); dorsal valve length 3.00 mm and width 2.36 mm on average; dorsal pseudointerarea with broad median groove and narrow propareas

https://doi.org/10.1017/jpa.2020.117 Published online by Cambridge University Press

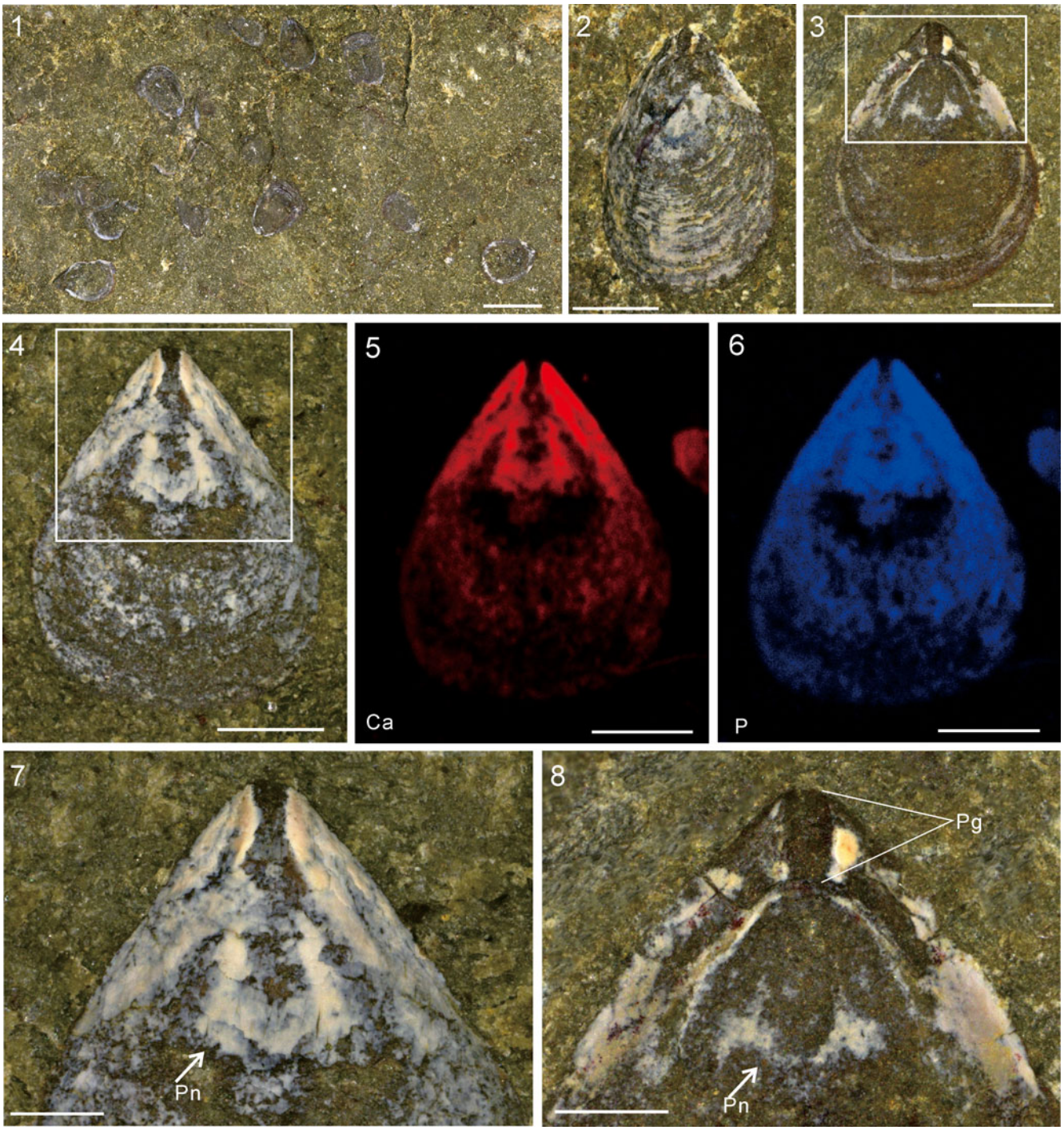

Figure 7. Ventral valves of the linguloid *Eoobolus malongensis* from the lower Cambrian Shipai Formation at Xiachazhuang section. (**1**) Shell concentrations (ELI QJP-SP-069); (**2**) ventral valve with concentric growth lines on the shell surface (ELI QJP-SP-163); (**3, 4**) ventral valves, (ELI QJP-SP-070, ELI QJP-SP-075); (**5, 6**) element maps of (**4**) investigated by micro X-ray fluorescence; (**7, 8**) close-up view of (**4**) and (**3**), respectively, showing pedicle groove (Pg) and 'U' shaped impression of pedicle nerve (Pn). Scale bars = 3 mm (**1**); or 1 mm (**2–6**); or 500 μm (**7, 8**).

(Fig. 8.6), occupying 22% of valve length and 72% of valve width; median tongue extending to 70% of valve length.

Materials.—Forty-eight specimens (including fragments) from middle-upper part of the Shipai Formation in the Xiachazhuang section.

Remarks.—Specimens from the Shipai Formation bear a strong resemblance to *Eoobolus malongensis*, described by Zhang et al (2020a) from the Cambrian Stage 4 Wulongqing Formation, Yunnan Province. *Eoobolus malongensis* from the Shipai Formation and Wulongqing Formation both have similar size ratios of several different morphologic characters in the ventral

https://doi.org/10.1017/jpa.2020.117 Published online by Cambridge University Press

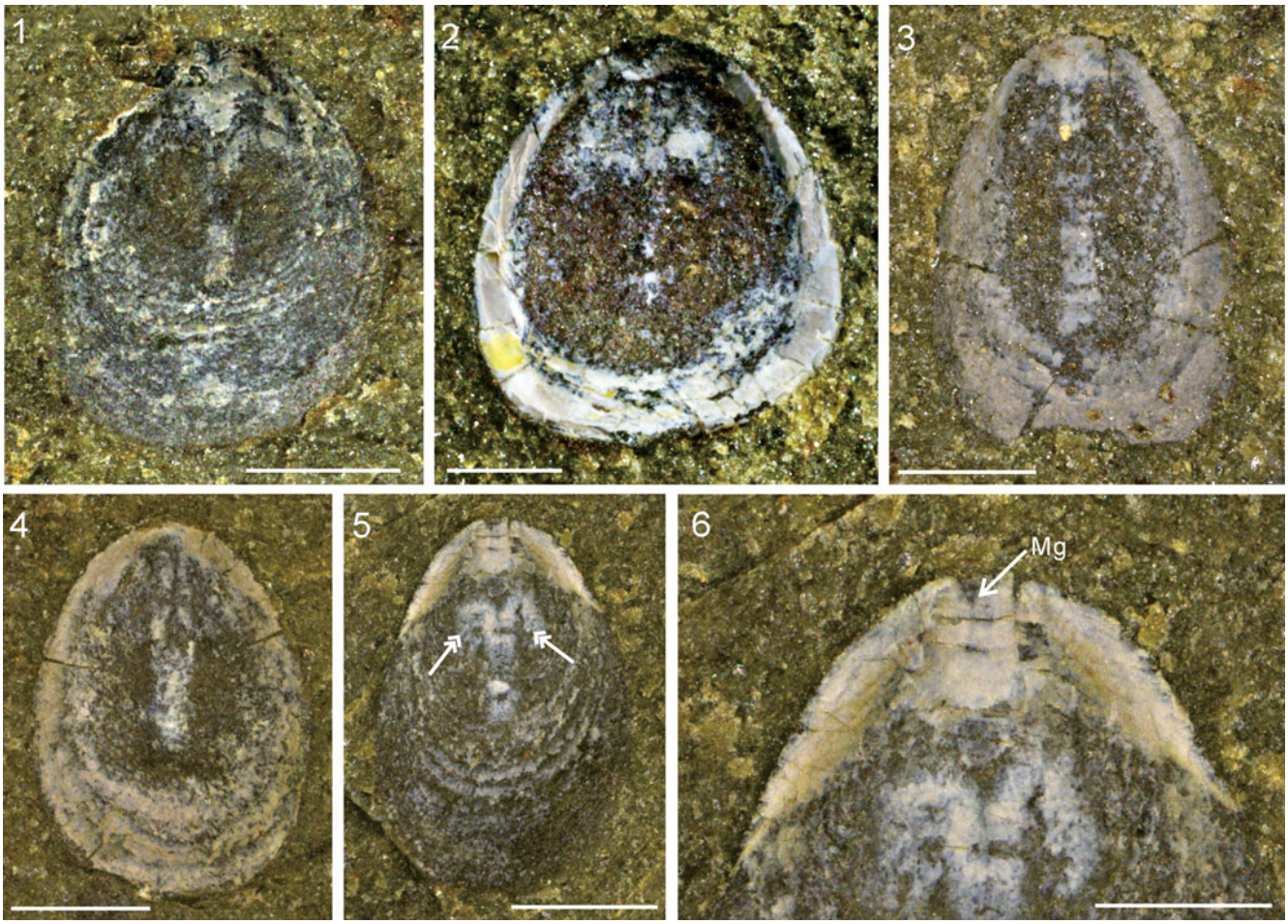

Figure 8. Dorsal valves of the linguloid *Eoobolus malongensis* from the lower Cambrian Shipai Formation at the Xiachazhuang section. (**1**) Dorsal valve with unambiguous and faint concentric growth lines on the shell surface (ELI QJP-SP-119); (**2–5**) dorsal valves with variable imprints of mantle canals (ELI QJP-SP-130, ELI QJP-SP-069-2, ELI QJP-SP-216-2, ELI QJP-SP-105) (marked by double arrows); (**6**) close-up view of (**5**) showing the triangular dorsal pseudointerarea with pronounced median groove (Mg, marked by arrow) and lateral propareas as ill-defined flexure lines. Scale bars = 1 mm (**1–6**).

valve (data from the Wulongqing Formation specimens: Aa = 74°, $L_p/L = 42\%$, $W_p/W = 78\%$, $Lpg/L = 18\%$; Zhang et al., 2020a; data of the specimens from the Shipai Formation in the Table 3). Relative warp analysis demonstrates strong similarities between *Eoobolus* from the Shipai and Wulongqing formations (Fig. 10), strengthening their taxonomic assignment to *Eoobolus malongensis* (Zhang et al., 2020a).

Eoobolus malongensis from the Shipai Formation can be distinguished from most of the species assigned to the genus in having a relatively narrow ventral pseudointerarea and a short pedicle groove with parallel lateral margins. It is also difficult to recognize any pustulose ornamentation on the postmetamorphic shell surface. However, comparison of shells from siliciclastic deposits to those acid-etched from carbonates is commonly a problem because taphonomic factors tend to alter morphological characters.

Family Neobolidae Walcott and Schuchert in Walcott, 1908
Neobolidae gen. indet. sp. indet.
Figure 11

Description.—Shell subcircular in outline (Fig. 11.1, 11.2), ~8.9 mm in length and ~9.7 mm in width; ~91% as long as wide. Dorsal median septum well developed, extending to mid-valve or two-thirds of valve length. Shell surface may have setae (marked by white arrow in SEM image, Fig. 11.3). Shell surface bears closely spaced concentric growth lines and dark speckled marks (Fig. 11.4), which are likely to be diagenetic mineral deposits with high concentration of Fe (Fig. 11.5); shell shows a strong elemental abundance of Ca, P, and S compared with the surrounding rock in the μ-XRF study (Fig. 11.6–11.8)

Materials.—Three dorsal valves from the middle-upper part of the Shipai Formation in the Xiachazhuang section.

Remarks.—Specimens from the Shipai Formation show a distinctive surface ornamentation with dense, regular concentric fila, and have a prominent dorsal median septum that indicates affinities with the Neobolidae. It is most similar to *Neobolus wulongqingensis* Zhang, Strotz, Topper, and Brock in Zhang et al., 2020b from the lower Cambrian Wulongqing Formation, eastern Yunnan (Zhang et al., 2020b), but without data on the ventral valve and more abundant materials, the discrimination of the material remains uncertain.

https://doi.org/10.1017/jpa.2020.117 Published online by Cambridge University Press

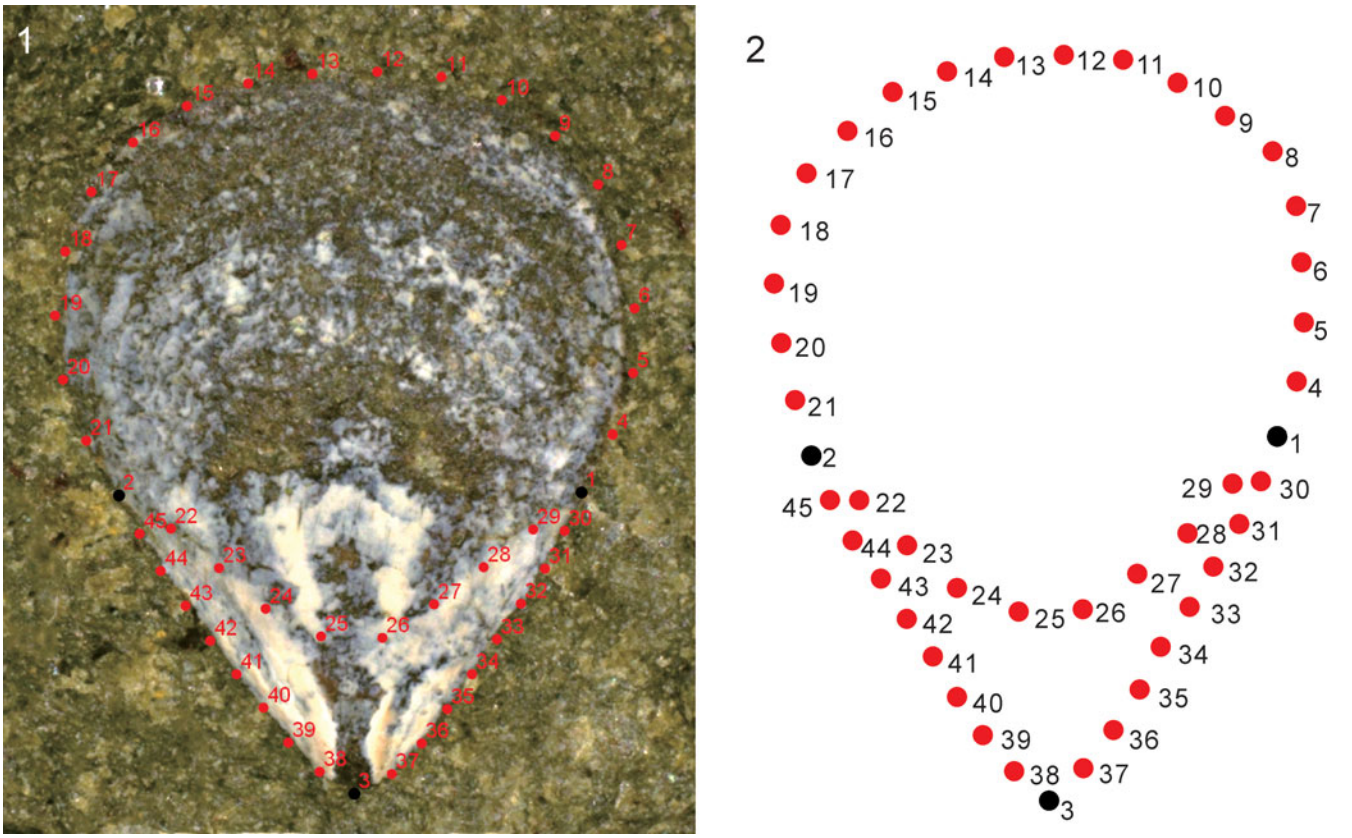

Figure 9. (**1, 2**) Definition of landmarks (marked by black circles) and semi-landmarks (marked by red circles).

Hence the specimens are referred to Neobolidae gen. indet. sp. indet. awaiting new data.

Subphylum Rhynchonelliformea Williams et al., 1996
Class Kutorginata Williams et al., 1996
Order Kutorginida Kuhn, 1949
Superfamily Nisusioidea Walcott and Schuchert in Walcott, 1908
Family Nisusiidae Walcott and Schuchert in Walcott, 1908
Genus *Nisusia* Walcott, 1905

Type species.—By original designation *Orthisina festinata* Billings, 1861, from unnamed Cambrian Stage 4 (*Bonnia-Olenellus* Zone) of USA and Canada.

Nisusia liantuoensis Zeng in Wang et al., 1987
Figure 12

1987 *Nisusia liantuoensis* Zeng in Wang et al., p. 213, pl. 9, figs. 13–16.
2008 *Nisusia liantuoensis*; Z.F. Zhang et al., p. 243, fig. 2c.

Holotype.—A ventral valve (LSP11-IV45951) from the Shipai Formation (unnamed Cambrian Series 2) of Liantuo, Yichang City, western Hubei Province, South China (Wang et al., 1987, pl. 9, fig. 15).

Emended diagnosis.—Shell subequally biconvex, semicircular to transverse-oval in outline; hinge line slightly shorter than or equal to the maximum width. Cardinal extremities slightly obtuse to almost rectangular. Ventral valve moderately convex, ventral umbo strongly raised; ventral interarea high, catacline. Dorsal valve with anacline interarea. Radial ornament with 6–11 ribs per 5 mm, rib crests bearing hollow spines.

Description.—Shell biconvex, sub-circular to transverse, sub-rectangular in outline, length about three-quarters of width. Hinge line equal to or slightly shorter than maximum shell width (~95% of the maximum width). Cardinal extremities form right angles. Shell surface bears numerous fine radial ribs that bifurcate in the adult phase to ~6–11 costae per 5 mm along the anterior margin.

Ventral valve semicircular or transversely sub-rectangular in outline, ~67% as long as wide; ventral valve moderately convex with the maximum height at the apex; apex pointed and raised, perforated by a round suproapical foramen (~0.54 mm in diameter) (Fig. 12.4, 12.5, marked by arrows). Ventral interarea high, with a triangular pseudodelthyrium occupying about one-third of interarea width (Fig. 12.4). Shell bears prominent radial lines and vague concentric lines; rib crests bearing hollow spines.

Dorsal valve subquadrate, ~78% as long as wide, with a small swelling at the umbo (Fig. 12.7–12.9); apex recurved

https://doi.org/10.1017/jpa.2020.117 Published online by Cambridge University Press

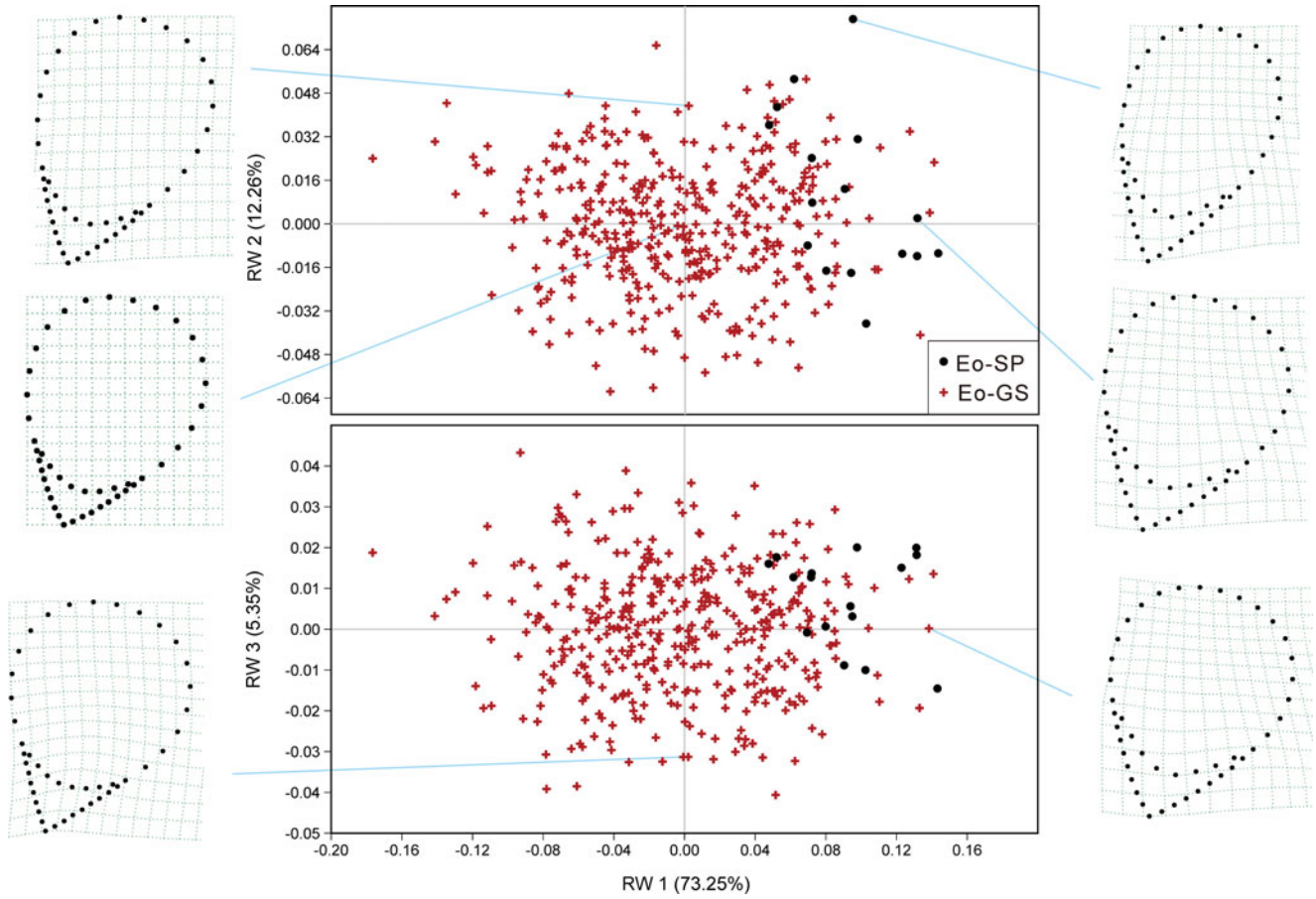

Figure 10. Plots for RW 1–2 and RW 1–3 of the relative warp analysis, with visualized shape of thin-plate splines within RW morphospace, showing the similarities of specimens of *Eoobolus* from the Guanshan fauna of eastern Yunnan (Eo-GS) with those from the Shipai Formation in Yichang area (Eo-SP), and signifying their assignment to *Eoobolus malongensis* (see Zhang et al., 2020a).

toward the posterior. Ornament on valve surface consists of radial costae and fine, closely set, concentric growth lines. Ventral and dorsal interior not observed.

Materials.—Seven ventral valves and five dorsal valves from the upper part of the Shipai Formation in the Xiachazhuang section. In addition, >10 specimens were also collected from the Shipai Formation from the Xiachazhuang section, but it is difficult to distinguish ventral or dorsal valves because all are incomplete shells.

Remarks.—*Nisusia liantuoensis* was first recorded from the Shipai Formation of Liantuo, Yichang City, South China (Zeng, 1987). Spinose ornament is unclear in Zeng (1987), hence Holmer et al. (2019) suggested this species designation may be questionable. Specimens from the Shipai Formation at Xiachazhuang section bear a strong resemblance to *N. liantuoensis* from Liantuo (shell subequally biconvex, semicircular in outline; ventral umbo strongly raised; ventral interarea high; the maximum height of the ventral valve at apex), and the new material from Xiachazhuang section also preserves the characteristic hollow spines of *Nisusia*.

Specimens from the Shipai Formation in the Xiachazhuang section are also similar to *Nisusia grandis* Roberts and Jell, 1990, from the Coonigan Formation (Wuliuan Stage) of western New South Wales; both have well-defined concentric lamellae and ventral valve interareas. But the new material differs from *Nisusia grandis* in having a rectimarginate anterior commissure and in lacking a ventral sulcus.

As discussed by Holmer et al. (2017, 2018), *Nisusia* has two pedicle openings, an apical foramen and a posterior median opening (between the delthyrium and notothyrium). *Nisusia liantuoensis* from the Shipai Formation shows a well-developed apical opening (Fig. 12.4, 12.5, marked by arrows) and bears a posterior median opening (Fig. 12.4, marked by double arrows). The new material is also similar to *Nisusia sulcata* Rowell and Caruso, 1985, from the Marjum Formation (Drumian) of western Utah, USA (Holmer et al., 2018, fig. 1B, E). However, *N. liantuoensis* differs in having the maximum height of the ventral valve at the apex rather than at the central part of the valve.

Superfamily Kutorginoidea Schuchert, 1893
Family Kutorginidae Schuchert, 1893
Genus *Kutorgina* Billings, 1861

Type species.—*Kutorgina cingulate* Billings, 1861, from lower Cambrian of Labrador, Canada.

Remarks.—*Kutorgina* holds special significance as it is one of the oldest brachiopods with a carbonate shell and primitive

https://doi.org/10.1017/jpa.2020.117 Published online by Cambridge University Press

Table 1. Main dimensions and ratios of ventral and dorsal valves of *Linnarssonia sapushanensis* from the lower Cambrian Shipai Formation in Three Gorges area. Abbreviations: V: ventral valve; D: dorsal valve; L, W: length and width of valve; L_a: length of ventral apical process; L_c, W_c: length and width of cardinal muscle scars; L_s: length of dorsal median septum. All measurements are in μm.

V	L	W	L_a	L_c	W_c	L/W	L_a/L	L_c/L	W_c/W	L_c/W_c
N	110	105	59	15	10	53	59	15	10	9
Mean	1688	1968	628	388	1036	86.17%	35.28%	22.40%	48.72%	40.20%
Max	2342	2730	869	470	1250	107.21%	42.65%	27.02%	55.06%	45.91%
Min	672	747	360	290	860	75.00%	26.21%	17.68%	43.31%	30.64%
SD	352	398	109	50	137	5.93%	4.51%	2.63%	3.12%	4.62%
D	L	W	L_s	L_c	W_c	L/W	L_s/L	L_c/L	W_c/W	L_c/W_c
N	82	82	71	42	44	77	70	42	42	38
Mean	1973	2070	1196	489	1074	95.32%	60.36%	25.09%	48.61%	46.95%
Max	2760	3138	1680	690	1545	171.15%	68.58%	40.93%	59.39%	57.02%
Min	1100	1040	657	324	722	81.64%	52.24%	19.31%	40.68%	40.40%
SD	342	401	208	80	169	13.20%	3.72%	4.61%	4.90%	4.45%

Table 2. Main dimensions and ratios of ventral valve of *Lingulellotreta ergalievi* from the lower Cambrian Shipai Formation in Three Gorges area. Abbreviations: V: ventral valve; L_p, W_p: length and width of ventral pseudointerarea; A: apical angle; All measurements are in μm.

V	L	W	L_p	W_p	A	L/W	L_p/L	W_p/W	L_p/W_p
N	6	5	5	5	5	5	5	5	5
Mean	4500	3370	1717	2505	69°	142.03%	37.40%	74.85%	68.78%
Max	5680	4000	2150	3160	73°	155.87%	40.26%	79.00%	84.64%
Min	3180	2470	1055	1870	60°	126.62%	33.17%	65.97%	48.50%
SD	1001	632	450	504	5°	10.84%	2.69%	6.10%	14.30%

Table 3. Main dimensions and ratios of ventral and dorsal valves of *Eoobolus malongensis* from the lower Cambrian Shipai Formation in Three Gorges area. Abbreviations: V: ventral valve; D: dorsal valve; L, W: length and width of valve; L_p, W_p: length and width of pseudointerarea; A: apical angle. All measurements are in μm.

V	L	W	L_p	W_p	A	L/W	L_p/L	W_p/W	L_p/W_p
N	32	32	15	14	15	32	15	14	14
Mean	3233	2449	1174	1790	78°	128.23%	36.90%	75.43%	63.33%
Max	4840	2969	1840	2190	87°	157.00%	46.00%	90.00%	86.00%
Min	2670	1915	725	1480	65°	121.00%	29.92%	56.00%	43.20%
SD	413	231	285	221	6°	8.00%	5.00%	8.00%	13.00%
D	L	W	L_p	W_p	L/W	L_p/L	W_p/W	L_p/W_p	
N	16	18	6	6	16	6	6	6	
Mean	2927	2361	628		1567				
					127.00%	22.00%	72.00%	41.00%	
Max	3942	3261	700		1838				
					156.00%	25.00%	75.00%	48.00%	
Min	2517	1660	524		1210				
					109.00%	19.00%	67.00%	31.00%	
SD	410	398	70	254	15.00%	2.00%	3.00%	7.00%	

articulation. *Kutorgina* had a cosmopolitan distribution during the early to middle Cambrian (Malakhovskaya, 2013), and has been recovered from China (Lu, 1979; Zhang et al., 2007b; Liu et al., 2015), Canada (Voronova et al., 1987), America (Nevada) (Walcott, 1905), Greenland (Skovsted and Holmer, 2005), Siberia (Gorjansky and Popov, 1985), Kazakhstan (Koneva, 1979), Kyrgyzstan (Popov and Tikhonov, 1990), and southeast Australia (Roberts and Jell, 1990). The wide geographic distribution of *Kutorgina* in the late early Cambrian may indicate that the larvae of *Kutorgina* were planktotrophic (Popov et al., 1997). Species of *Kutorgina* have few distinctive characters, and morphological features vary throughout ontogeny. The kutorginides may be easily recognized by the wide posterior margin, coarse external concentric ornamentation of sharp rugae and ridges, and growth lines following the valve outline (Malakhovskaya, 2013). Specimens from the Shipai Formation in the Three Gorges area with coarse, wide-spaced concentric growth lines clearly belong in *Kutorgina*.

Kutorgina sinensis Rong in Lu, 1979
Figure 13

1979 *Kutorgina sinensis* Rong in Lu, p. 72, pl. v, figs. 9–11.
1987 *Iphidella*? *liantuoensis*; Zeng, p. 213, pl. 8, figs. 14–18.

Holotype.—A ventral valve from the lower Cambrian Xinji Formation, Shuiyu section, Ruicheng, Shanxi (Lu, 1979, pl. v, fig. 9).

Emended diagnosis.—Shell sub-trapezoid, with rounded anterior and lateral margins; shell width is somewhat shorter than shell length, hinge line about three-fifths of the shell width. Ventral valve moderately convex, interarea apsacline; umbo slightly raised over the posterior margin; sulcus narrow, shallow, and starts from the postmedian part of the valve. The ornamentation consists of concentric growth lamellae (~18–20 lamellae over the entire shell).

Description.—Shell biconvex, rounded to sub-pentagonal. Shell surface ornamented with coarse, widely spaced concentric growth lamellae that are best developed on the postmedian part of the valve, no visible prominent micro-ornamentation. The distance between growth lamellae is 0.64 mm on average. Ventral valve rounded to sub-pentagonal in outline (Fig. 13.1–13.5), with rounded anterior and lateral margins. The ratio of shell length to width ranges from 0.84–1.10 (average 0.92). Dorsal valve moderately convex to semicircular in outline (Fig. 13.6–13.8), ~73% as long as wide. Umbo small and slightly raised over the posterior margin (Fig. 13.8). SEM shows external shell with pyrite crystals (Fig, 13.9, 13.10). No information on the internal morphology is preserved.

Materials.—Thirty-four specimens comprising 14 ventral valves, six dorsal valves, and fragments, all from the upper part of the Shipai Formation at Xiachazhuang section.

https://doi.org/10.1017/jpa.2020.117 Published online by Cambridge University Press

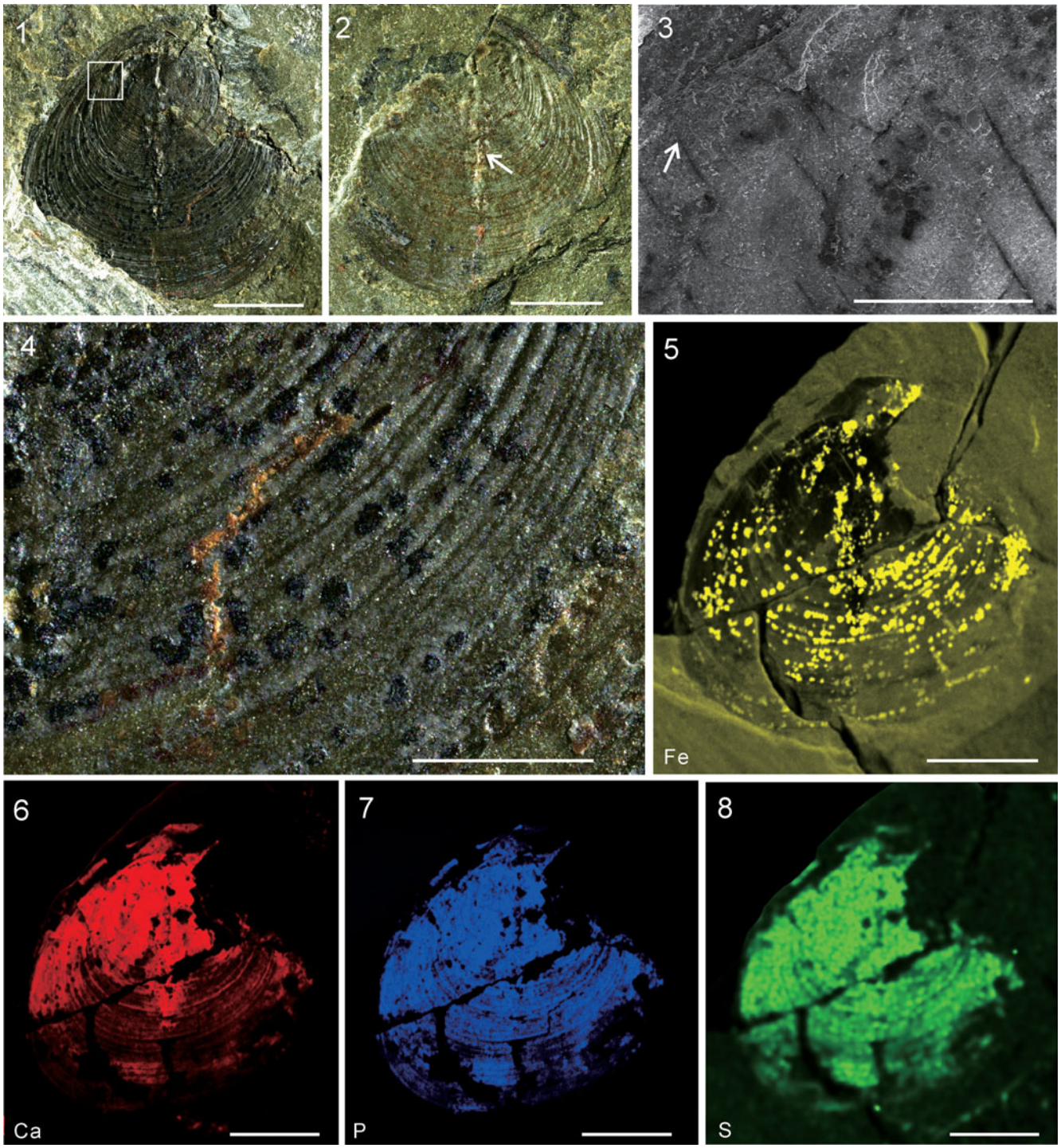

Figure 11. Neobolidae gen. indet. sp. indet. from the lower Cambrian Shipai Formation at Xiachazhang section. (**1, 2**) Part and counterpart of Neobolidae gen. indet. sp. indet. with prominent dorsal median septum (marked by arrow) (ELI QJP-SP-001A, ELI QJP-SP-001B); (**3**) SEM image of (**1**) marked by the inset box, showing possible setae (marked by white arrow); (**4**) close-up view of (**1**) showing concentric growth lines of the shell surface; (**5–8**) micro-XRF mapping, showing the rich content of Fe on the shell dark speckled marks (**5**) and the concentration Ca, P, and S on the shell (**6–8**). Scale bars = 3 mm (**1, 2, 5–8**), or 1 mm (**3, 4**).

Remarks.—The holotype of *Kutorgina sinensis* Rong in Lu, 1979 from the lower Cambrian Xinji Formation in North China was illustrated by Lu (1979), but was not described in detail. Figured material from Lu (1979) shows that the ventral valve is moderately convex, ~13 mm wide, with an apsacline interarea. New material from the Shipai Formation is similar to *K. sinensis* Rong in Lu, 1979 from the Xinji Formation (Lu, 1979). Both have a moderately convex ventral valve, similar shell size (shell width of Shipai Formation specimens ranges from 6–14 mm), as well as concentric growth lamellae (ranging from 18–20 lamellae). However, *K. sinensis* from the Xinji Formation is represented by a single ventral valve with

https://doi.org/10.1017/jpa.2020.117 Published online by Cambridge University Press

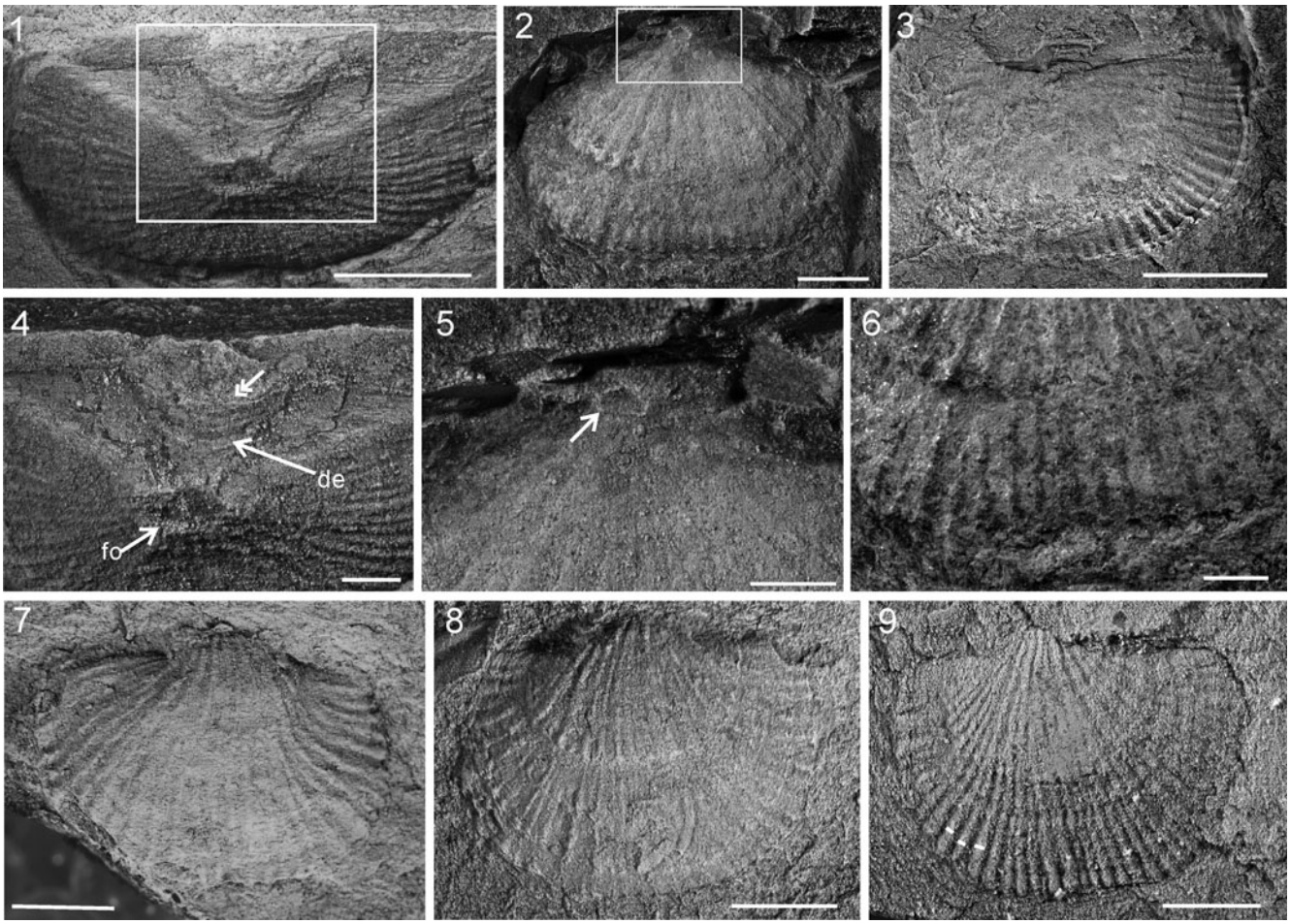

Figure 12. *Nisusia liantuoensis* from the lower Cambrian Shipai Formation at Xiachazhuang section. (**1**) Posterior view of ventral valve (ELI QJP-SP-015); (**2, 3**) ventral valves (ELI QJP-SP-045, ELI QJP-SP-006); (**4**) close-up view of (**1**) showing the apical foramen (fo, marked by arrow), developed pseudointerarea, deltidium (de, marked by arrow), and posterior median opening (marked by double arrows); (**5**) an enlargement of (**2**), showing the pedicle foramen (marked by arrow); (**6**) a fragment of one ventral valve, showing the radial lines on the shell surface (ELI QJP-SP-045); (**7–9**) dorsal valves (ELI QJP-SP-037, ELI QJP-SP-013, ELI QJP-SP-008). Scale bars = 3 mm (**1, 7–9**), 2 mm (**2**), 4 mm (**3**), or 1 mm (**4–6**).

no information about the morphology of the dorsal valve, so comparisons of these features is difficult.

Kutorgina sinensis from the Shipai Formation bears some similarities with *K. chengjiangensis* Zhang et al., 2007b from the Yu'anshan Formation of South China (Zhang et al., 2007b), which is also recovered as "crack-outs" from siliciclastic deposits. Both have strong concentric growth lamellae, as well as other closely comparable morphology, such as shell size (*K. chengjiangensis*: L = 9.70 mm, W = 11.12 mm on average, data from Zhang et al., 2007b; *K. sinensis*: L = 9.40 mm, W = 11.02 mm on average), and the distance between growth lines (*K. chengjiangensis*: 0.6–0.8 mm; *K. sinensis*: ~0.64 mm on average). However, *K. sinensis* from the Shipai Formation has a more convex and acuminate ventral valve as compared with *K. chengjiangensis*.

In addition, *Kutorgina chengjiangensis* from the Chengjiang Lagerstätte features a stout and annulated pedicle previously described as protruding from between the delthyrium and notothyrium (Zhang et al., 2007b). However, recent reexamination shows that the pedicle emerges from the apical foramen (Holmer et al., 2018). Unfortunately, *K. sinensis* from the Shipai Formation are preserved as exterior molds without soft tissues, which precludes detailed study of the pedicle morphology. Additionally, study of the apical foramen is problematic due to poor preservation of the ventral apex.

Kutorgina sp.
Figure 14

Description.—Shell planoconvex or slightly biconvex, up to 14 mm wide; surface ornamented by concentric growth lines. No median sulcus or fold developed in the shell valve. Ventral valve transversely oval or semicircular with rounded anterior and lateral margins. Posterior of ventral valve not well preserved. Dorsal valve almost flat and slightly convex, ~75% as long as wide; posterior margin almost straight, and slightly shorter than the maximum shell width (located in the middle of the shell). No information on the internal morphology is preserved.

Materials.—Seven specimens comprising three ventral valves and four dorsal valves, all from the upper part of the Shipai Formation in the Xiachazhuang section.

https://doi.org/10.1017/jpa.2020.117 Published online by Cambridge University Press

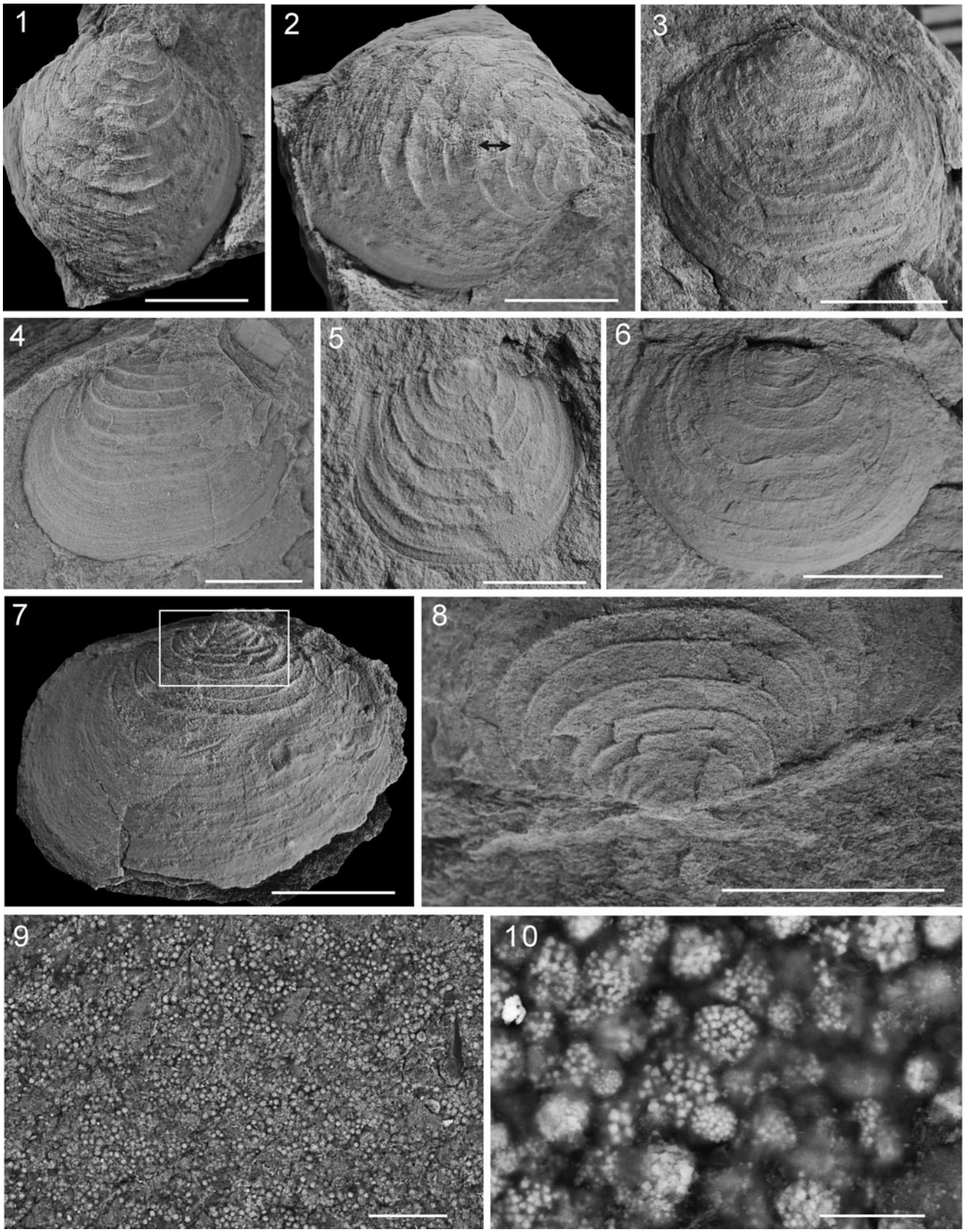

Figure 13. *Kutorgina sinensis* from the lower Cambrian Shipai Formation at Xiachazhuang section. (**1**) Ventral valve (ELI QJP-SP-007); (**2**) lateral view of (**1**), note the distance between growth lines (marked by double-pointed arrow); (**3–5**) ventral valves (ELI QJP-SP-013, ELI QJP-SP-076, ELI QJP-SP-078); (**6, 7**) dorsal valves (ELI QJP-SP-014, ELI QJP-SP-012); (**8**) close-up view of (**7**) showing small umbo located posterior of the posterior margin; (**9**) SEM image of (**1**) showing pyrite crystals; (**10**) close-up view of (**9**). Scale bars = 5 mm (**1–4, 6–8**), 3 mm (**5**), 100 μm (**9**), or 10 μm (**10**).

https://doi.org/10.1017/jpa.2020.117 Published online by Cambridge University Press

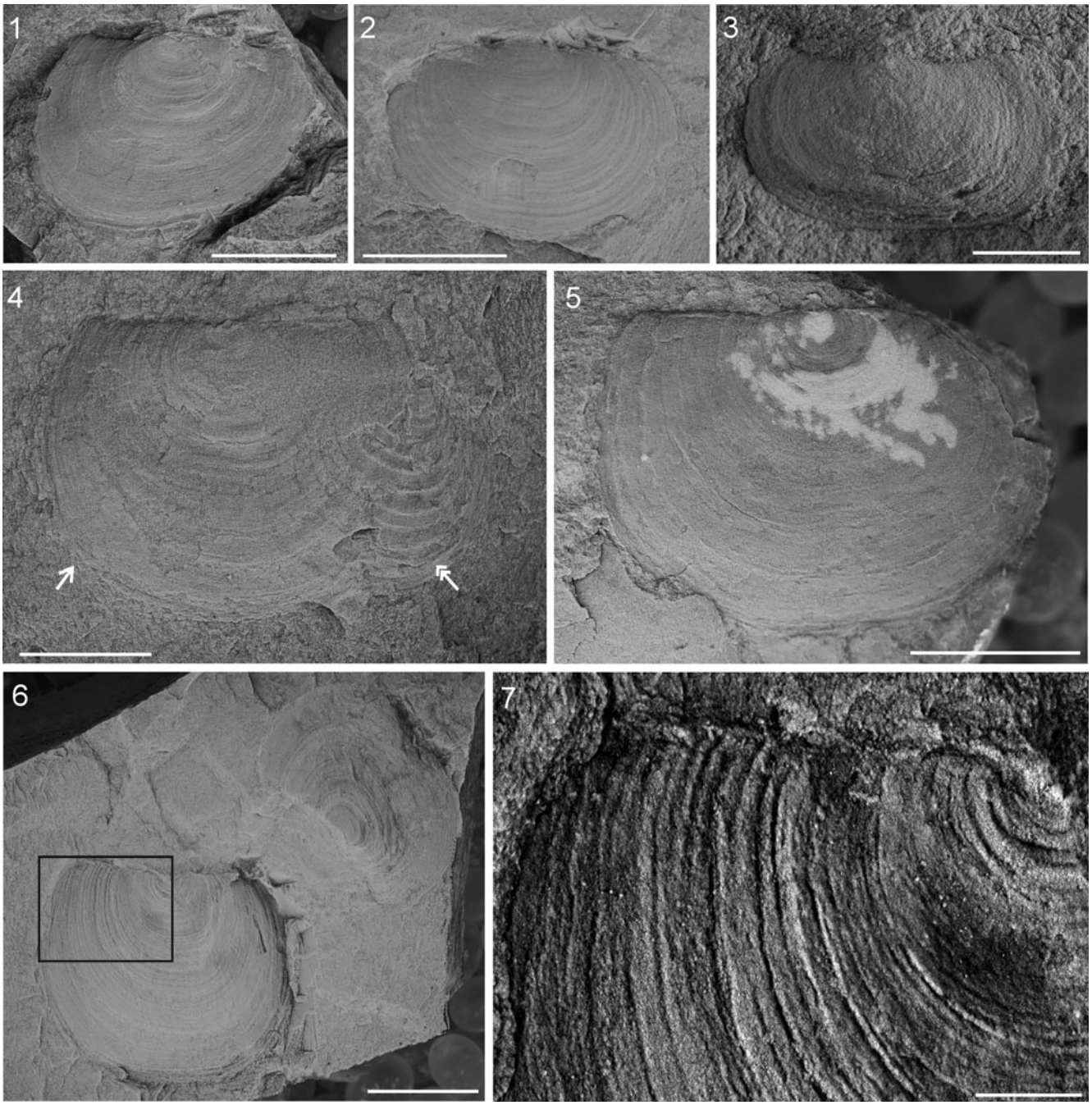

Figure 14. *Kutorgina* sp. from the lower Cambrian Shipai Formation at Xiachazhuang section. (**1–3**) Ventral valves (ELI QJP-SP-065, ELI QJP-SP-035, ELI QJP-SP-017); (**4**) dorsal valve of *Kutorgina* sp. (ELI QJP-SP-032, marked by arrow) and an fragment of *K. sinensis* (marked by double arrows); (**5, 6**) dorsal valves (ELI QJP-SP-049, ELI QJP-SP-074); (**7**) close-up view of (**6**), showing the concentric growth lines. Scale bars = 5 mm (**1, 2**, **4–6**), 2 mm (**3**), or 1 mm (**7**).

Remarks.—*Kutorgina* sp. has a similar shell size as *K. sinensis*, but it can be distinguished from *K. sinensis* by the ornamentation and shell shape. *Kutorgina sinensis* is ornamented with concentric growth lamellae (~5–7 lamellae per 5 mm), while *Kutorgina* sp. has 10–15 concentric growth lines per 5 mm. *Kutorgina* sp. is similar to *K. reticulata* Poulsen, 1932 (Skovsted and Holmer, 2005) in having transversely oval or semicircular outline, almost flat dorsal valve with a straight posterior margin, and shell surface with concentric growth lines. But it differs in lacking developed dorsal median fold and ventral median sulcus. Further detailed comparison is difficult due to insufficient material available for the study.

Brachiopod assemblages from the Shipai Formation

Xiachazhuang section.—Brachiopod assemblages from the Xiachazhuang section are much more abundant and diverse compared to those from the Aijiahe and Wangjiaping sections. Six hundred thirteen slabs with >4000 *Linnarssonia sapushanensis* valves have been recovered from the Shipai

https://doi.org/10.1017/jpa.2020.117 Published online by Cambridge University Press

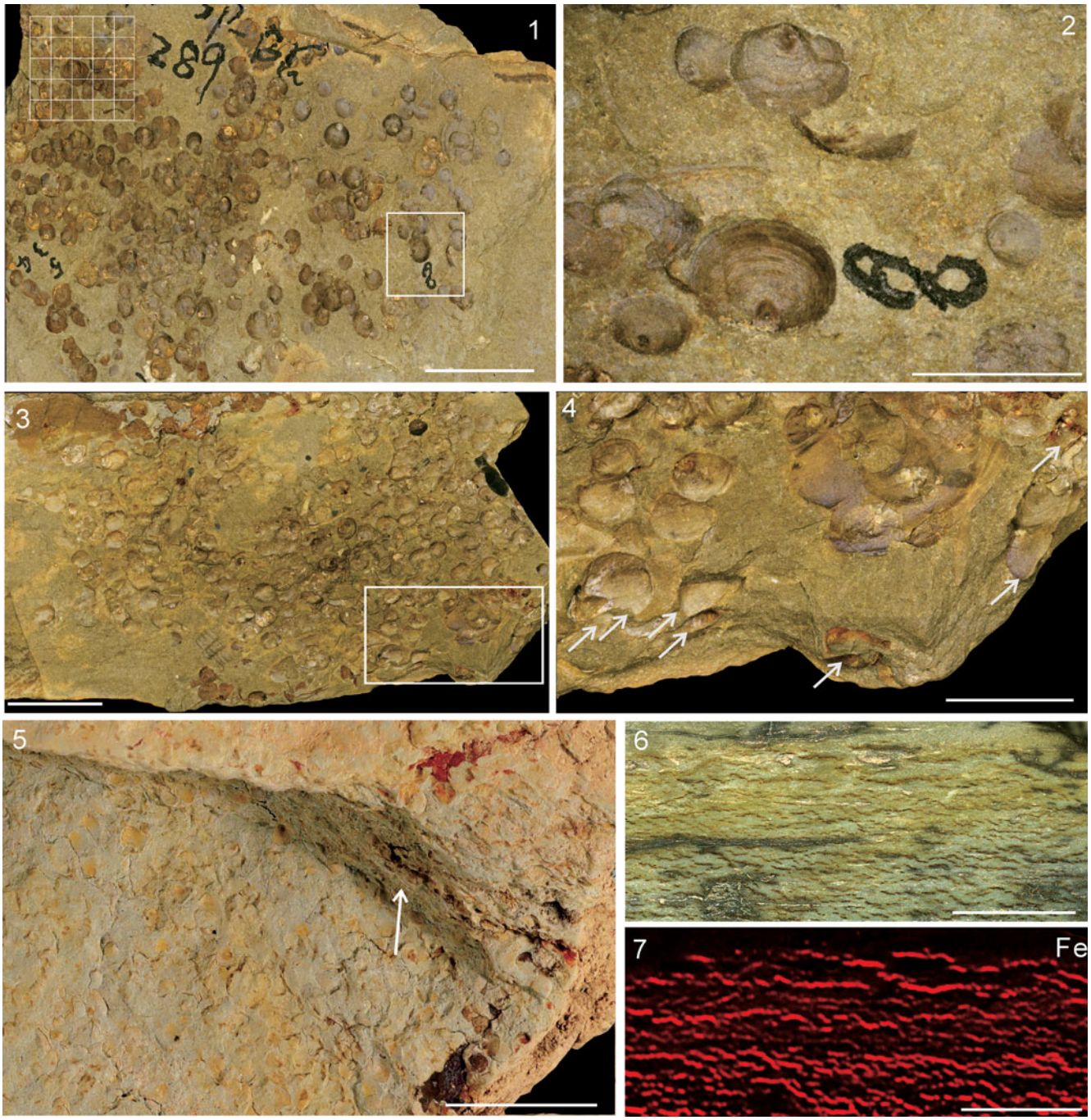

Figure 15. Acrotretoid brachiopod shell concentrations of *Linnarssonia sapushanensis* from the lower Cambrian Shipai Formation at Xiachazhuang section of Hubei Province, and comparison to shell beds of *L. sapushanensis* from the Wulongqing Formation of Yunnan Province. (**1–4**) Acrotretoid shell concentrations from the Shipai Formation; (**1**) shell valves aggregated as high-density concentrations on the bedding plane (ELI QJP-SP-289), with inset box indicating the position of (**2**) and grid in upper left used to count the number of shells in 1 cm^2; (**2**) close-up view of (**1**) showing acrotretoid shell valves of different sizes distributed on the bedding plane; (**3**) acrotretoid shell bed (ELI QJP-SP-357); (**4**) close-up view of (**3**) marked by an inset box, showing the acrotretoid shell valves distributed at different micro-layers of bedding planes (marked by white arrows); (**5**) multi-layered, high-density shell beds from Wulongqing Formation packed up to 2 cm thick (ELI SJJ-164); (**6**) longitudinally polished section of (**5**), showing frequent occurrences of the acrotretoid shell valves, aggregated approximately as 11–13 pavements within 1 cm thick muddy sediment; (**7**) micro-XRF mapping of (**6**), showing the rich content of Fe within the acrotretoids. Scale bars = 1 cm (**1, 3, 5–7**), 3 mm (**2**), 4 mm (**4**).

Formation in the Three Gorges area. Most fossils were collected from the silty mudstone and siltstone in the middle to upper part of the Shipai Formation, ~120 m above the base. Here, *Linnarssonia sapushanensis* are commonly aggregated as shell concentrations on the same bedding plane (Fig. 15.1–15.4). These shell beds range from loosely to densely packed (~18 valves per 1 cm^2) (Fig. 15.1) with moderate degrees of fragmentation. In the *L. sapushanensis* shell beds in the Xiachazhuang section, the size frequency distribution of 103 shells shows that individuals with shell widths between 1.23–

https://doi.org/10.1017/jpa.2020.117 Published online by Cambridge University Press

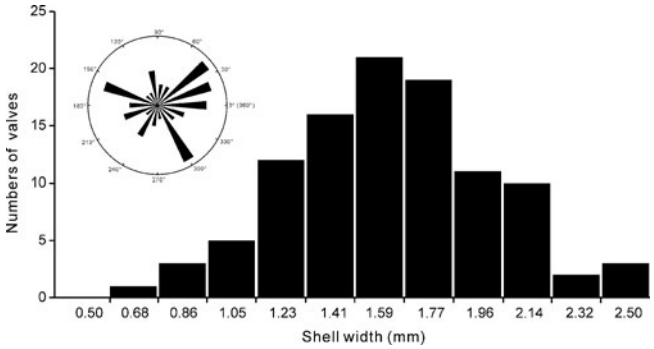

Figure 16. Size frequency distribution and rose diagram of *Linnarssonia sapushanensis* from the lower Cambrian Shipai Formation at Xiachazhuang section, Three Gorges area, South China.

2.10 mm are the most frequent (up to 86%) (Fig. 16). The orientation angle of the shells of *L. sapushanensis* was also statistically analyzed and plotted in a rose diagram, showing that they have random orientations (Fig. 16). Many shells retain well-preserved microstructures.

Linguloid brachiopods are quite common in the Shipai Formation, and two species have been recognized: *Lingulellotreta ergalievi* and *Eoobolus malongensis*. The majority of the linguloid specimens were collected from the siltstone in the middle-upper part of the Shipai Formation, ~150 m above the base of the Shipai Formation (Fig. 1.3). *Eoobolus malongensis*, which is the most common species in this unit, is preserved as individuals or shell concentrations (Figs. 7, 8). All specimens of *E. malongensis* are flattened and compressed, but retain

Figure 17. The acrotretoid brachiopod of *Linnarssonia sapushanensis* and fragmental trilobite *Palaeobolus liantuoensis* from the lower Cambrian Shipai Formation at Aijiahe section, Three Gorges area, South China. (**1–3**) Acrotretoids (marked by white arrows) with fragmental trilobites distributed on the bedding plane (ELI AJH-SP-130, ELI AJH-SP-119, ELI AJH-SP-110); (**4, 5**) ventral valves (ELI AJH-SP-110-1, ELI AJH-SP-170); (**6, 7**) dorsal valves (ELI AJH-SP-109, ELI AJH-SP-097). Scale bars = 4 mm (**1**), 2 mm (**2**), 6 mm (**3**), or 500 μm (**4–7**).

https://doi.org/10.1017/jpa.2020.117 Published online by Cambridge University Press

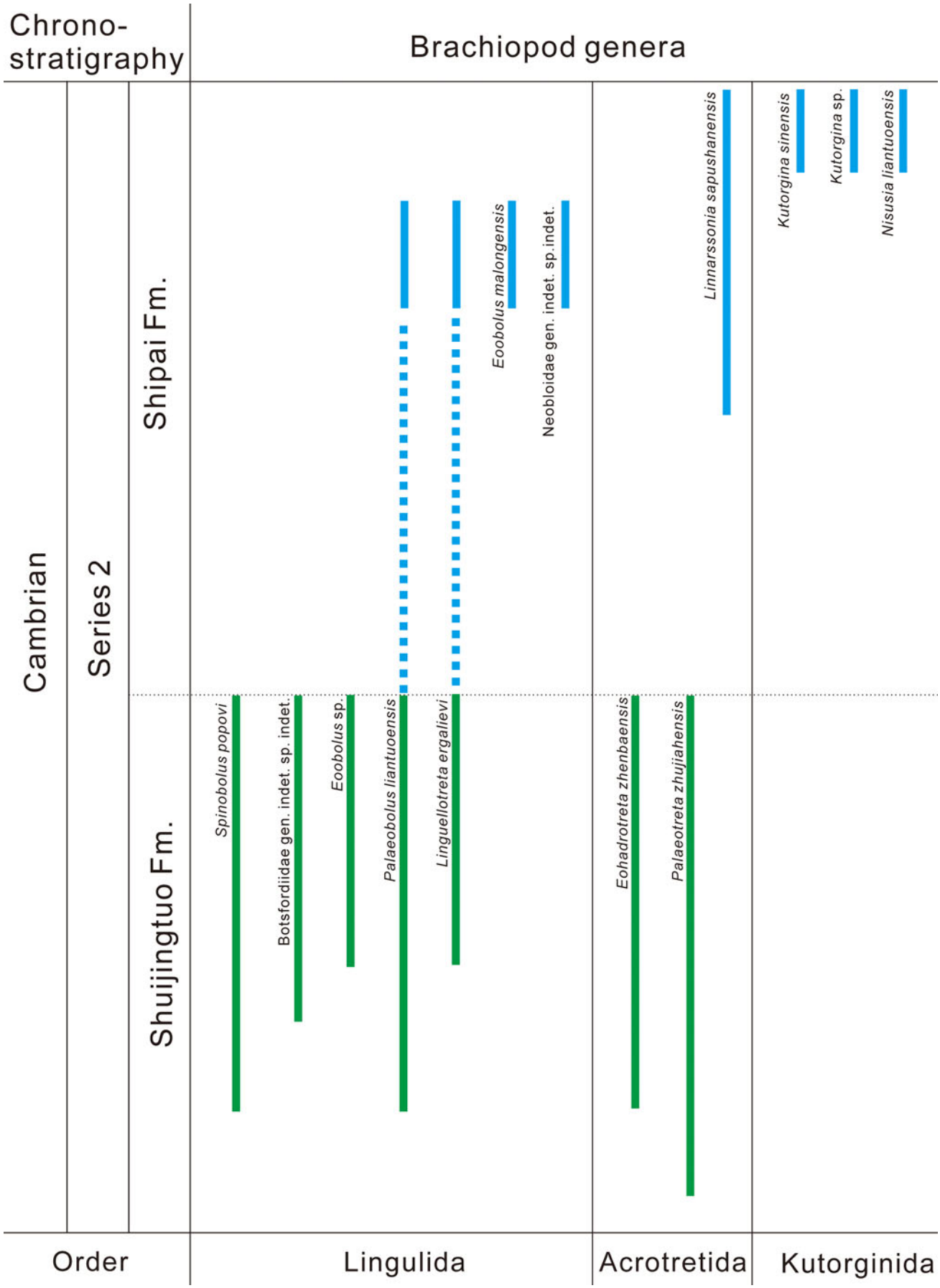

Figure 18. The stratigraphical ranges of brachiopods that occur in the Three Gorges area, South China.

https://doi.org/10.1017/jpa.2020.117 Published online by Cambridge University Press

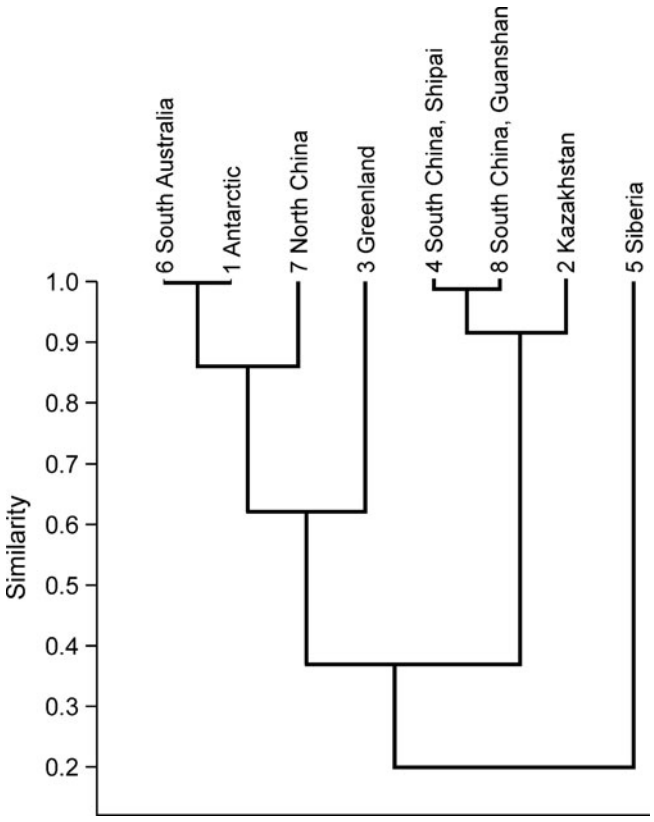

Figure 19. Results of the pair-group cluster analysis for the Cambrian Stage 4 linguliform genera from 8 localities (Raup-Crick similarity).

some vague concentric growth lines. Overall morphology, including the pseudointerarea of the specimens illustrated herein, is similar to the linguloid brachiopods from the Guanshan fauna (Wulongqing Formation) (Zhang et al., 2020a). In the Shipai Formation, *Lingulellotreta ergalievi* is relatively rare, has a longer ventral pseudointerarea than *Eoobolus malongensis*, and has an elongate, oval-shaped pedicle foramen. In this unit, *Eoobolus* and *Lingulellotreta* are usually <5 mm wide and long. However, the *Eoobolus*-yielding level in the Shipai Formation also includes larger macro-morphic brachiopods, generally ~10 mm wide (8.9 mm in length and 9.7 mm in width) (Fig. 11).The shell surface of the macro-morphic brachiopods bears closely spaced concentric growth lines, and a prominent dorsal median septum is present (Fig. 11.2). The specimens (Fig. 11) are most similar to brachiopods belonging to Neobolidae, but the limited material precludes more robust taxonomic discrimination.

In the top silty shale of the Shipai Formation, ~200 m above the base of the Shipai Formation (Fig. 1.3), the fauna is dominated by calcareous-shelled kutorginates (*Nisusia liantuoensis*, *Kutorgina sinensis*, and *Kutorgina* sp.). All specimens of *Kutorgina* have a distinctive shell ornamentation, and are sub-pentagonal or semicircular with strongly spaced concentric growth lines on the surface of the shell. *Nisusia* has prominent radial lines and has strikingly similar morphology to those from the Wulongqing Formation (Guanshan fauna), eastern Yunnan (Hu et al., 2013; Li et al., 2017). In South China, the first appearance datum (FAD) of the rhynchonelliform *Nisusia* is in the upper silty shale of the Shipai and Wulongqing formations.

Aijiahe and Wangjiaping sections.—The Wangjiaping section is the type section of the Shipai fauna (Zhang and Hua, 2005) and is exposed around the northern bank of the Yangtze River near Wangjiaping Village, ~40 km west of Yichang City (Fig. 1.2). Presently, the Shipai Formation at the Wangjiaping section is poorly exposed and mostly covered, making new collections difficult. Linguloid brachiopods such as *Palaeobolus*, *Eoobolus*, and *Lingulellotreta* have been reported from the argillaceous siltstone and silty mudstone in the middle part of the Shipai Formation in the Wangjiaping and Aijiahe sections (Zhang et al., 2015). The brachiopod assemblage in the Aijiahe section consists mainly of acrotretoid brachiopods, which is similar to that from the Xiachazhuang section. Acrotretoids collected from the silty mudstone in the middle-upper part of the Shipai Formation in the Aijiahe section are usually preserved as individuals or shell concentrations (brachiopod-trilobite) (Fig. 17). Four specimens of *Eoobolus malongensis* have been recovered from the brick-red silty mudstone in the top of the Shipai Formation in the Aijiahe section. All the individuals of *E. malongensis* were preserved as flattened internal molds with similar color to the surrounding muddy matrix.

Discussion

Early Cambrian brachiopod assemblages in South China.—Brachiopod faunas from the lower Cambrian Shuijingtuo Formation in the Three Gorges area include four linguloids (*Spinobolus popovi* Zhang and Holmer in Z.F. Zhang et al., 2016, *Eoobolus* sp., *Lingulellotreta ergalievi*, and *Palaeobolus*? *liantuoensis* Zeng, 1987), one botsfordiid (Botsfordiidae gen. indet. sp. indet.), and two acrotretoids (*Eohadrotreta zhenbaensis* Li and Holmer, 2004 and *Palaeotreta zhujiahensis* Li and Holmer, 2004) (Z.F. Zhang et al., 2016; Z.L. Zhang et al., 2020). Notably, *Palaeotreta* from the base of the Shuijingtuo Formation in the Xiaoyangba section of southern Shaanxi Province is the oldest acrotretoid known from the carbonate deposits in South China (Li and Holmer, 2004; Z.F. Zhang et al., 2016; Z.L. Zhang et al., 2016, 2018a, b, 2020). They are typified by lacking both an internal pedicle tube and apical pits in the ventral valve interior. The overlying Shipai Formation contains linguloids (*Palaeobolus liantuoensis*, *Lingulellotreta ergalievi*, *Eoobolus malongensis*, and Neobolidae gen. indet. sp. indet.), an acrotretoid (*Linnarssonia sapushanensis*) and calcareous shelled Kutorginates (*Nisusia liantuoensis*, *Kutorgina sinensis*, *Kutorgina* sp.) (Fig. 18). Acrotretoids (represented by *Linnarssonia sapushanensis*) are numerically abundant in the siliciclastic rocks from the Shipai Formation, and also constitute the dominant taxon (including *Eohadrotreta zhenbaensis*, *Palaeotreta zhujiahensis*) in the carbonate rocks from the Shuijingtuo Formation. In addition, the occurrence of the calcareous brachiopods *Kutorgina* and *Nisusia* in the Shipai Formation may represent the earliest records of this group in the Three Gorges area.

In the light of evidence on the Guanshan biota (Wulongqing Formation) recovered from the siliciclastic rocks of eastern Yunnan of China (Luo et al., 2008; Hu et al., 2013), it is clear

https://doi.org/10.1017/jpa.2020.117 Published online by Cambridge University Press

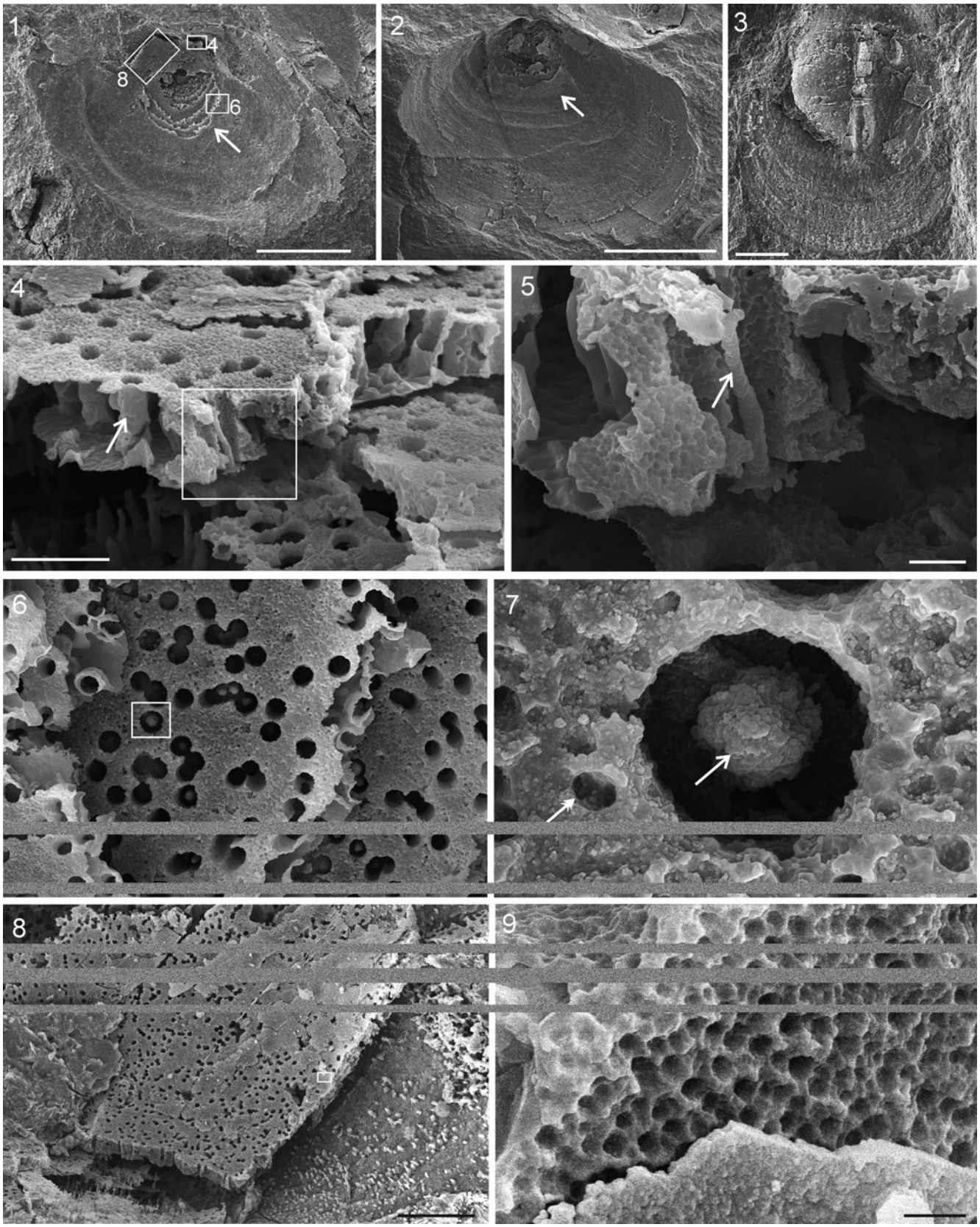

Figure 20. SEM images of acrotretoid *Linnarssonia sapushanensis* showing the secondary shell structure. (**1, 2**) Internal view of ventral valves (ELI QJP-SP-205-1, ELI QJP-SP-205-2), arrows indicate apical process; (**3**) internal view of dorsal valve (ELI QJP-SP-205-4); (**4**) the column structure; (**5**) enlarged view of (**4**) marked by the inset box, showing the hollow tube (marked by arrow) with a solid column (marked by arrow); (**6**) vertical view of columnar structure; (**7**) enlargement of (**6**), showing the circular pit on the interlaminar surface (marded by arrow on left) and external aperture of the hollow tube with a solid structure (marked by arrow on right) in vertical view; (**8**) columnar structure, showing the hollow tube openings on the exposed interlaminar surfaces of the secondary shell layer; (**9**) close-up view of (**8**), showing the circular pits on the interlaminar surface. Scale bars = 500 μm (**1**), 1 mm (**2, 3**), 10 μm (**4, 6**), 2 μm (**5**), 1 μm (**7, 9**), or 50 μm (**8**).

https://doi.org/10.1017/jpa.2020.117 Published online by Cambridge University Press

Table 4. Previous studies of brachiopod column structure from dissolved limestone.

Taxon	Dimension (μm)	Chronology	Stratigraphy	Locality	Reference
Acrotretida	average 3	middle Cambrian	Swasey Limestone	Topaz Mountains, Utah	Holmer, 1989
Prototreta attenuata					
Angulotreta	range 1.5–5	upper Cambrian	Riley and Wilberns formations	central Texas, US	Williams and Holmer, 1992
Vandalotreta fragilis	average 4	middle Cambrian	Jbel Wawrmast Formation	Morocco	Streng, 1999
Monophthalma cf. *M. eggegrundensis*	range 2–3	middle Cambrian	Jbel Wawrmast Formation	Morocco	Streng, 1999
Almohadella braunae	range 2–3	middle Cambrian	Jbel Wawrmast Formation	Morocco	Streng, 1999
Eohadrotreta zhenbaensis	average 2.5	lower Cambrian	Shuijingtuo Formation	South China	Z.L. Zhang et al., 2016
Lingulida:	range 3–5	lower Cambrian	Shabakty Group	Kazakhstan	Cusack et al., 1999
Linguellotreta sp.					
Kyrshabaktella sp.	range 2–3.5	lower Cambrian	Harkless Formation	Nevada	Skovsted and Holmer, 2006
?*Canalilatus simplex*	range 1.5–2	middle Cambrian	Forsemölla Limestone Bed	southern Sweden	Streng et al., 2008
Eoobolus? sp. aff. *E. priscus*	range 1.5–2.2	middle Cambrian	Forsemölla Limestone Bed	southern Sweden	Streng et al., 2008

that the assemblage belongs to Cambrian Age 4 fossil brachiopods. Early Cambrian brachiopods from eastern Yunnan are highly diverse and abundant. *Diangdongia pista* Rong, 1974 occurs in the black bioclastic siltstone of the basal Yu'anshan Formation (*Parabadiella* Biozone) and is one of the oldest brachiopods in South China (Z.F. Zhang et al., 2003, 2008). Brachiopods diversified during Series 2, Stage 3 (*Wudingaspis-Eoredlichia* Biozone), and many additional brachiopod taxa are documented from the silty shales of the Yu'anshan Formation, including linguliforms such as *Eoglossa chengjiangensis* Jin, Hou, and Wang, 1993, *Lingulellotreta yuanshanensis*, and *Xianshanella haikouensis* Zhang and Han, 2004, rhynchonelliforms *Kutorgina chengjiangensis*, *Alisina* sp., and *Longtancunella chengjiangensis* Hou et al., 1999, and stem-group brachiopods *Heliomedusa orienta* Sun and Hou, 1987 and *Yuganotheca elegans* Zhang et al., 2014 (Zhang and Holmer, 2013; Hou et al., 2017; Li et al., 2017; Chen et al., 2019; Liang et al., 2020; Zhang et al., 2020a). The acrotretoid *Kuangshanotreta malungensis* Zhang, Holmer, and Hu in Wang et al., 2012 occurs in the upper siltstone of the Yu'anshan Formation (Wang et al., 2012). In eastern Yunnan, brachiopod assemblages in the Hongjingshao Formation (Cambrian Series 2, Stage 4) are dominated by *Palaeobolus yunnanensis* Rong, 1974. Overall, brachiopod faunas in eastern Yunnan tend to be less abundant and diverse in the Duyunian, most likely due to the large amplitude eustatic changes that resulted in a major regression (evident between the Hongjingshao and Wulongqing formations) (Li et al., 2017; Zhu et al., 2019). In contrast, brachiopod assemblages associated with the Guanshan Biota in the overlying Wulongqing Formation (Cambrian Stage 4) are abundant and diverse (Luo et al., 2008; Hu et al., 2013). Eight brachiopod genera are reported from the Wulongqing Formation including *Linnarssonia*, *Eoobolus*, *Neobolus*, *Schizopholis*, *Acanthotretella*, *Palaeobolus*, *Kutorgina*, and *Nisusia* (which occurs in the *Palaeolenus* Biozone) (Hu, 2005; Hu et al., 2013; Zhang and Holmer, 2013; Zhang and Shu, 2014; Zhang et al., 2015, 2020a, b; Li et al., 2017; Chen et al., 2019).

Regional correlations of the Shipai Formation.—Absolute age of the Shipai Formation is poorly resolved. However, two trilobite biozones have been recognized in the Shipai Formation: the *Redlichia meitanensis* Zone in the lower parts of the succession and the *Palaeolenus lantenosis* Zone in the upper parts (Zhang et al., 1980; Wang et al., 1987; Zhang and Hua, 2005; X.L. Zhang et al., 2008). This indicates an age of Cambrian Stage 4, similar to the Wulongqing Formation in eastern Yunnan (Wang et al., 1987; Zhang et al., 2015). Brachiopods—particularly linguliform brachiopods (linguloids and acrotretoids)—from the Shipai Formation also corroborate a Cambrian Stage 4 age for the Shipai Formation (Z.F. Zhang et al., 2016). Brachiopods from Cambrian Stage 4 are presently known from all main continents, including South Australia, Antarctic, Greenland, Kazakhstan, Siberia, and China (Pelman, 1977; Holmer et al., 2001; Ushatinskaya and Malakhovskaya, 2001; Skovsted and Holmer, 2005; Betts et al., 2016, 2017, 2019; Chen et al., 2019; Pan et al., 2019; Ushatinskaya and Korovnikov, 2019; Claybourn et al., 2020; Zhang et al., 2020a, b). Cluster analysis of Cambrian, Stage 4 linguliforms shows that the faunas from South China (Shipai Formation, Guanshan biota) and Kazakhstan cluster together (Fig. 19). This is defined by the occurrence of *Eoobolus*, *Palaeobolus*, *Lingulellotreta*, and *Linnarssonia*. Clustering of east Antarctica, South Australia, and North China is consistent with the biostratigraphic correlation of Claybourn et al. (2020) based on brachiopods.

The brachiopod fauna from the Shipai Formation is dominated by the acrotretoid *Linnarssonia sapushanensis*, which are commonly aggregated as patchy concentrations of shell valves on the same bedding plane (Fig. 15.1–15.4), notably in the Xiachazhuang section. In contrast, the acrotretoids from the Wulongqing Formation form thicker shell beds (~11–13 pavements within a 1 cm thick bed) (Fig. 15.5–15.7). Differential accumulation styles of acrotretoid valves highlight differences between sedimentary paleoenvironments and energy regimes of the Shipai and Wulongqng formations. In the Wulongqing Formation of eastern Yunnan, where acrotretoid brachiopod shells form dense stacks, the shells were probably affected by high energy currents, and were briefly suspended before their final deposition on the sea floor. In contrast, acrotretoidshell beds from the Shipai Formation in the Hubei Province are characterized by lower density shell concentrations, probably the result of deposition in a deeper environment where current energy was minimal.

Similarities between *Linnarssonia* shell beds in the middle Shipai Formation in the Three Gorges area and the lower to middle Wulongqing Formation in Wuding area, eastern Yunnan suggest that these two successions may be roughly correlated. This is further corroborated by the first appearance datum (FAD) of the rhynchonelliform calcareous-shelled brachiopod *Nisusia* in the silty mudstone of both the Shipai and Wulongqing formations.

https://doi.org/10.1017/jpa.2020.117 Published online by Cambridge University Press

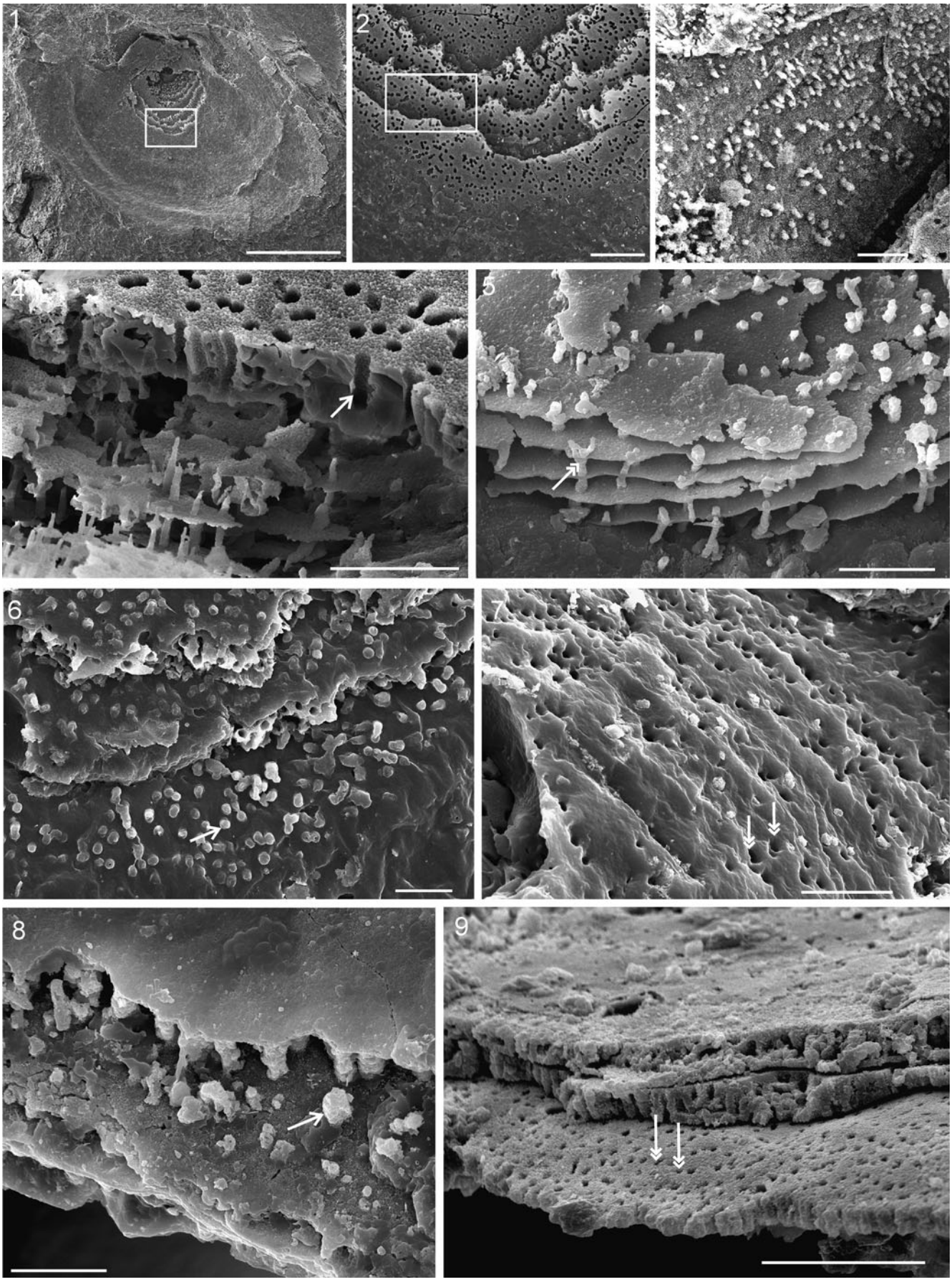

https://doi.org/10.1017/jpa.2020.117 Published online by Cambridge University Press

Figure 21. Comparison of the acrotretoid secondary shell layer from different depositional environments. (**1**) Internal view of ventral valves (ELI QJP-SP-205-1); (**2, 3**) close-up view of (**1**); (**4**) close-up view of columnar structure, note the hollow tube (marked by arrow); (**5**) the thin solid columns that connected the laminae; (**6, 7**) latex casts of (**2, 3**) showing the secondary columnar structure of an acrotretoid from the Shipai Formation (siliciclastic deposits); (**8, 9**) secondary columnar structure of an acrotretoid from the Shuijingtuo Formation (carbonate deposits) showing the columns (marked by arrow) with central canals (marked by double arrows) (ELI BE-AJH 201502-013, ELI BE-AJH 201502-014). Scale bars = 500 μm (**1**), 100 μm (**2**), 20 μm (**3, 4, 6, 7, 9**), or 10 μm (**5, 8**).

Shell structures of acrotretoid brachiopods from fine siliciclastics.—Organophosphatic brachiopod shells usually consist of an organic periostracum, a mineralized laminar primary layer, and a secondary columnar layer (Holmer, 1989; Williams and Holmer, 1992; Williams et al., 1997; Holmer et al., 2008; Streng et al., 2008). The thin organic periostracum is usually exfoliated during taphonomic processes. The primary layer is generally very thin, usually not much more than 1 μm thick, and is easily lost during transportation and burial, resulting in the exposure of the secondary layer (Williams and Holmer, 1992; Williams et al., 1997). The secondary layer is mainly composed of an alternating arrangement of lamina and columns. The columnar shell structure is characteristic of acrotretid brachiopods (Holmer, 1989; Williams and Holmer, 1992), but has been demonstrated to occur in several lingulid brachiopods, including Lingulellotretidae, Dysoristidae, and Kyrshabaktellidae (Cusack et al., 1999; Skovsted and Holmer, 2006). Similar shell structures are also present in *Canalilatus* (Streng et al., 2008), the stem lineage of brachiopods *Mickwitzia* (Skovsted and Holmer, 2003; Holmer et al., 2008), *Micrina* (Williams and Holmer, 2002), and the tommotiid *Tannuolina* (Skovsted et al., 2014).

Although the shell structure of acrotretoid brachiopods is well known from examples preserved in carbonate deposits (Poulsen, 1971; Popov and Ushatinskaya, 1986; Rowell, 1986;

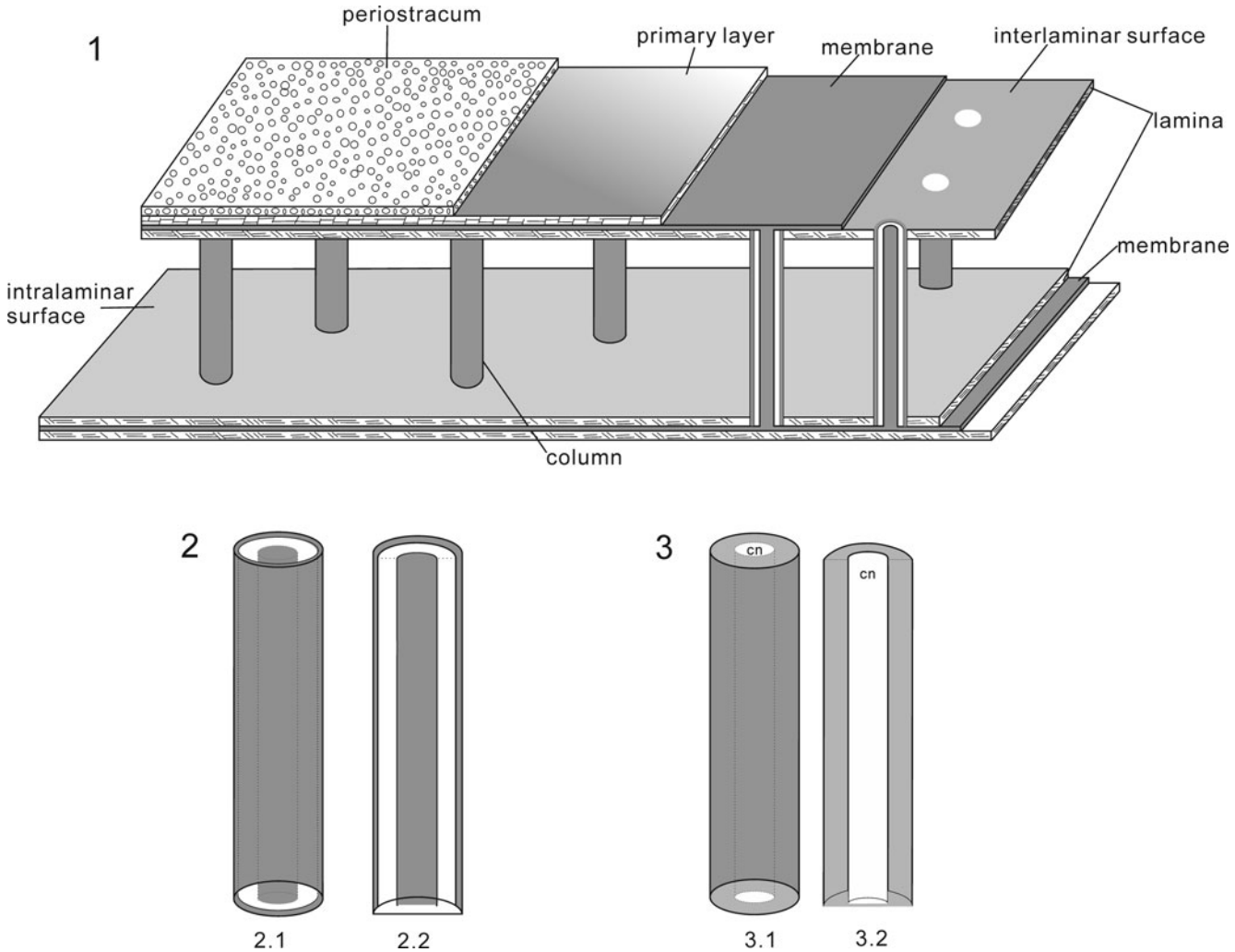

Figure 22. (**1**) Diagrammatic reconstruction of shell structure of the acrotretoid brachiopods, illustrating relationships between successive discrete shell layers (modified from Williams and Holmer, 1992; Williams et al., 2000); (**2**) column structure from the mudstone (gray indicates solid structure), sketch of Figure 20.4-20.5, showing the hollow tube with a solid column (2.1), and the longitudinal section of the hollow tube (2.2); (**3**) column structure from the dissolving limestone (gray indicates solid structure), sketch of Figure 21.8–21.9, showing the column with a central canal (cn) (3.1), and the longitudinal section of a column (3.2).

https://doi.org/10.1017/jpa.2020.117 Published online by Cambridge University Press

Ushatinskaya et al., 1988; Holmer, 1989; Williams and Holmer, 1992; Holmer et al., 2008; Z.L. Zhang et al., 2016), no details of acrotretoid shell structures preserved in siliciclastic rocks have ever been described. Most acrotretoids in muddy deposits are preserved as internal molds (e.g., Duan et al., 2021), which precludes investigation of shell structural details (Mergl and Kordule, 2008; Mergl, 2019). However, specimens of the acrotretoid *Linnarssonia* from the silty mudstone of the Shipai Formation have well-preserved shell ultrastructures, allowing detailed study of the acrotretoid shell ultrastructure from siliciclastic deposits for the first time.

The primary layer forming the ornamentation of the external shell surface (e.g., concentric fila) is preserved in some specimens of *L. sapushanensis* from the Shipai Formation (Fig. 2.1). The secondary layer is also well developed, and has a columnar structure that is mainly composed of hollow tubes (diameter = 2.5 μm on average, range 1.6–3.8 μm), with solid columns (~1 μm in diameter) that are composed of stacks of pinacoidal plates (Fig. 20.4, 20.5). The hollow tubes in *L. sapushanensis* are comparable morphologically with those previously documented in other acrotretoid brachiopods, such as *Anglulotreta* (1.5–5 μm diameter) (Table 4) (Holmer, 1989; Williams and Holmer, 1992; Streng, 1999; Streng and Holmer, 2006; Streng et al., 2008; Z.L. Zhang et al., 2016). The solid columns in the tubes (Fig. 20.5) and the solid columns that connected the laminae (Fig. 21.5) are comparable with those columnar central canals (~1 μm in diameter) (Fig. 21.9). Latex casts of these hollow tubes and thin solid columns in *L. sapushanensis* (Fig. 21.6, 21.7) also provide detailed molds for comparison with acid-etched material (Fig. 21.8, 21.9).

It is generally accepted that the empty intralaminar spaces in acrotretoid shells originally contained an organic matrix, and that the slots between successive laminae and columnar canals were originally occupied by sheets and strands, respectively composed of proteins or chitin (Poulsen, 1971; Ushatinskaya et al., 1988; Holmer, 1989; Williams and Holmer, 1992). In *L. sapushanensis* from the Shipai Formation, the intralaminar spaces are commonly empty, thus exposing the hollow tubes in relief (Fig. 20.4), but occasionally the spaces are filled with mineralized materials (Fig. 21.4). The interlaminar surfaces of lamellae are ornamented with circular pits (Fig. 20.7, 20.9) and hollow tube openings (Fig. 20.8), usually ~500 nm and 2.5 μm, respectively. The hollow tubes may have contained unmineralized organic fibers that were lost post-mortem. Thus, the hollow tube and solid column of the acrotretoid column structure from the Shipai Formation could be the equivalent of the traditional column and central canal structure observed in shells dissolved from limestone (Fig. 22).

Conclusion

This is the first comprehensive description of the brachiopod faunas and their systematic diversity from the Shipai Formation (Stage 4) in the Three Gorges area of South China. This assemblage includes the representatives of the subphylum Linguliformea: linguloids (*Lingulellotreta ergalievi*, *Eoobolus malongensis*, and Neobolidae gen. indet. sp. indet.), an acrotretoid (*Linnarssonia sapushanensis*), and calcareous-shelled rhynchonelliforms (*Kutorgina sinensis*, *Kutorgina* sp., and *Nisusia liantuoensis*). Cluster analysis of linguliform, Cambrian Stage 4 brachiopods shows that the faunas of South China (Shipai Formation and the Wulongqing Formation) group closely with those from Kazakhstan.

The brachiopod fauna from the Shipai and Wulongqing formations both include the rhynchonelliform *Nisusia*, and preserve shell concentrations of the acrotretoid *L. sapushanensis*. In the Shipai Formation, *L. sapushanensis* are preserved in patchy aggregations on the same bedding plane, whereas in the Wulongqing Formation they form thick shell beds. This suggests that the Wulongqing Formation represents a slightly higher energy paleoenvironment than the quieter Shipai Formation.

In siliciclastics, brachiopods are commonly preserved as casts and molds and retention of shell material is generally rare. Brachiopods from the Shipai Formation however, retain shell material, the remarkable preservation of which is possibly due to deposition in a low energy paleoenvironment. *Linnarssonia sapushanensis* from the Shipai Formation has a hollow tube and solid column microstructure, which is likely to be the equivalent of traditional column and central canal-type microstructure often observed in acid-etched acrotretids. Knowledge of shell microstructures in Cambrian acrotretoids is primarily derived from specimens acid etched from limestones. This study provides the first detailed description of acrotretoid shell structures from Cambrian siliciclastics, providing an important comparison with acid-etched material.

Acknowledgments

We are grateful to C. Zabini, M. Mergl, and the Journal Associate Editor C.D. Sproat for their constructive comments and suggestions. Financial support from the National Natural Science Foundation of China (41890844, 41425008, 41621003, and 41720104002 to ZZF) and the 111 project (D17013) for continuous fossil collectioning of Xi'an group are sincerely acknowledged. L.E. Holmer's work was supported by a grant from the Swedish Research Council (VR 2018-03390). Many thanks to the early fossil collections organized by the workingteam at the Early Life Institute (NWU), and joined by J.P. Zhai, F.Y. Chen, Z.L. Zhang, X.R. Wang, and H.Z. Wang working therein.

Accessibility of supplemental data

Data available from the Dryad Digital Repository: https://doi.org/10.5061/dryad.2ngf1vhmn.

References

Bassett, M.G., Popov, L.E., and Holmer, L.E., 1999, Organophosphatic brachiopods: patterns of biodiversification and extinction in the early Palaeozoic: Geobios, v. 32, p. 145–163.

Betts, M.J., Paterson, J.R., Jago, J.B., Jacquet, S.M., Skovsted, C.B., Topper, T.P., and Brock, G.A., 2016, A new lower Cambrian shelly fossil biostratigraphy for South Australia: Gondwana Research, v. 36, p. 176–208.

Betts, M.J., Paterson, J.R., Jago, J.B., Jacquet, S.M., Skovsted, C.B., Topper, T.P., and Brock, G.A., 2017, Global correlation of the early Cambrian of South Australia: shelly fauna of the *Dailyatia odyssei* Zone: Gondwana Research, v. 46, p. 240–279.

Betts, M.J., Paterson, J.R., Jacquet, S.M., Andrew, A.S., Hall, P.A., Jago, J.B., Jagodzinski, E.A., Preiss, W.V., Crowley, J.L., Brougham, T., Mathewson,

https://doi.org/10.1017/jpa.2020.117 Published online by Cambridge University Press

C.P., García-Bellido, D.C., Topper, T.P., Skovsted, C.B., and Brock, G.A., 2018, Early Cambrian chronostratigraphy and geochronology of South Australia: Earth-Science Reviews, v. 185, p. 498–543.
Betts, M.J., Claybourn, T.M., Brock, G.A., Jago, J.B., Skovsted, C.B., and Paterson, J.R., 2019, Shelly fossils from the lower Cambrian White Point Conglomerate, Kangaroo Island, South Australia: Acta Palaeontologica Polonica, v. 64, p. 489–522.
Billings, E., 1861, Palaeozoic fossils containing descriptions and figures of new or little known species of organic remains from the Silurian rocks: Geological Survey of Canada, v. 1, p. 1–24.
Carlson, S.J., 2016, The evolution of Brachiopoda: Annual Review of Earth and Planetary Sciences, v. 44, p. 409–438.
Chang, S., Feng, Q., Clausen, S., and Zhang, L., 2017, Sponge spicules from the lower Cambrian in the Yanjiahe Formation, South China: the earliest biomineralizing sponge record: Palaeogeography, Palaeoclimatology, Palaeoecology, v. 474, p. 36–44.
Chang, S., Feng, Q., and Zhang, L., 2018, New siliceous microfossils from the Terreneuvian Yanjiahe Formation, South China: the possible earliest radiolarian fossil record: Journal of Earth Science, v. 29, p. 912–919.
Chen, F.Y., Zhang, Z.F., Betts, M.J., Zhang, Z.L., and Liu, F., 2019, First report on Guanshan Biota (Cambrian Stage 4) at the stratotype area of Wulongqing Formation in Malong County, eastern Yunnan, China: Geoscience Frontiers, v. 10, p. 1459–1476.
Chen, X., Rong, J.Y., Fan, J.X., Zhan, R.B., Mitchell, C.E., Harper, D.A.T., Melchin, M.J., Peng, P.A., Finney, S.C., and Wang, X.F., 2006, The Global Boundary Stratotype Section and Point (GSSP) for the base of the Hirnantian Stage (the uppermost of the Ordovician System): Episodes, v. 29, p. 183–195.
Claybourn, T.M., Skovsted, C.B., Holmer, L.E., Pan, B., Myrow, P.M., Topper, T.P., and Brock, G.A., 2020, Brachiopods from the Byrd Group (Cambrian Series 2, Stage 4) central Transantarctic Mountains, east Antarctica: biostratigraphy, phylogeny and systematics: Papers in Palaeontology, p. 1–35.
Cobbold, E.S., 1921, The Cambrian horizons of Comley (Shropshire), and their Brachiopoda, Pteropoda, Gastropoda, etc: Quarterly Journal of the Geological Society of London, v. 76, p. 325–386.
Cusack, M., Williams, A., and Buckman, J.O., 1999, Chemico-structural evolution of linguloid brachiopod shells: Palaeontology, v. 42, p. 799–840.
Dai, T., and Zhang, X.L., 2011, Ontogeny of the Eodiscoid Trilobite *Tsunyidiscus acutus* from the lower Cambrian of South China: Palaeontology, v. 54, p. 1279–1288.
Dawson, J.W., 1868, Acadian Geology; the geological structure, organic remains, and mineral resources of Nova Scotia, New Brunswick, and Prince Edward Island: London, Macmillan, 694 p.
Duan, X.L., Liang, Y., Holmer, L.E., and Zhang, Z.F., 2021, First report of acrotretoid brachiopod shell beds in the lower Cambrian (Stage 4) Guanshan Biota of eastern Yunnan, South China: Journal of Paleontology, v. 95, p. 40–55. https://doi.org/10.1017/jpa.2020.66.
Fu, D.J., Tong, G.H., Dai, T., Liu, W., Yang, Y.N., Zhang, Y., Cui, L.H., Li, L.Y., Yun, H., Wu,Y., Sun, A., Liu, C., Pei, W.R., Gaines, R.R., and Zhang, X.L., 2019, The Qingjiang biota—a Burgess Shale-type fossil Lagerstätte from the early Cambrian of South China: Science, v. 363, p. 1338–1342.
Gorjansky, V., and Koneva, S.P., 1983, Lower Cambrian inarticulate brachiopods of the Malyi Karatau Range (southern Kazakhstan): Trudy Instituta Geologii i Geofiziki, Akademiya Nauk SSSR, Sibirskoe Otdelenie, v. 541, p. 128–138. [in Russian]
Gorjansky, V., and Popov, L.E., 1985, Morphology, systematic position and origin of inarticulate brachiopods with a carbonate shell: Paleontologicheskii Zhurnal, v. 3, p. 3–14. [in Russian]
Guo, J.F., Li, Y., Han, J., Zhang, X.L., Zhang, Z.F., Ou, Q., Liu, J.N., Shu, D.G., Maruyama, S., and Komiya, T., 2008, Fossil association from the lower Cambrian Yanjiahe Formation in the Yangtze Gorges area, Hubei, South China: Acta Geologica Sinica (English Edition), v. 82, p. 1124–1132.
Guo, J.F., Li, Y., and Li, G.X., 2014, Small shelly fossils from the early Cambrian Yanjiahe Formation, Yichang, Hubei, China: Gondwana Research, v. 25, p. 999–1007.
Hammer, Ø., Harper, D.A.T., and Ryan, P.D., 2001, PAST: Paleontological statistics software package for education and data analysis: Palaeontologia Electronica, v. 4, p. 1–9.
Harper, D.A., Popov, L.E., and Holmer, L.E., 2017, Brachiopods: origin and early history: Palaeontology, v. 60, p. 609–631.
Holmer, L.E., 1989, Middle Ordovician phosphatic inarticulate brachiopods from Västergötland and Dalarna, Sweden: Fossils and Strata, p. 1–172.
Holmer, L.E., and Popov, L.E., 2000, Lingulata, *in* Kaesler, R.L., ed., Treatise on Invertebrate Paleontology, Part H, Brachiopoda, Volume 2: Boulder, Colorado and Lawrence, Kansas, Geological Society of America and University of Kansas Press, p. H30–H146.
Holmer, L.E., Popov, L.E., and Wrona, R., 1996, Early Cambrian lingulate brachiopods from glacial erratics of King George Island (South Shetland Islands), Antarctica, *in* Gaździcki, A., ed., Palaeontological Results of the Polish Antarctic Expeditions. Part 2: Palaeontologia Polonica, v. 55, p. 37–50.
Holmer, L.E., Popov, L.E., Koneva, S.P., and Rong, J.Y., 1997, Early Cambrian *Lingulellotreta* (Lingulata, Brachiopoda) from south Kazakhstan (Malyi Karata Range) and South China (eastern Yunnan): Journal of Paleontology, v. 71, p. 577–584.
Holmer, L.E., Popov, L.E., Koneva, S.P., and Bassett, M.G., 2001, Cambrian–Early Ordovician brachiopods from Malyi Karatau, the western Balkash region, and northern Tien Shan, Central Asia: Special Papers in Palaeontology, v. 65, p. 1–180.
Holmer, L.E., Popov, L.E., and Streng, M., 2008, Organophosphatic stem group brachiopods - implications for the phylogeny of the Subphylum Linguliformea: Fossils and Strata, v. 54, p. 3–11.
Holmer, L.E., Zhang, Z.F., Topper, T.P., Popov, L., and Claybourn, T.M., 2017, The attachment strategies of Cambrian kutorginate brachiopods: the curious case of two pedicle openings and their phylogenetic significance: Journal of Paleontology, v. 21, p. 33–39.
Holmer, L.E., Popov, L.E., Pour, M.G., Claybourn, T.M., Zhang, Z.L., Brock, G.A., and Zhang, Z.F., 2018, Evolutionary significance of a middle Cambrian (Series 3) in situ occurrence of the pedunculate rhynchonelliform brachiopod *Nisusia sulcata*: Lethaia, v. 51, p. 425–432.
Holmer, L.E., Kebria-ee Zadeh, Mohammad-Reza, Popov, L.E., Ghobadi Pour, M., Álvaro, J., Hairapetian, V., and Zhang Z.F., 2019, Cambrian rhynchonelliform nisusioid brachiopods: phylogeny and distribution: Papers in Palaeontology, v. 5, p. 559–575.
Hou, X.G., Bergström, J., Wang, H.F., Feng, X.H., and Chen, A.L., 1999, The Chengjiang Fauna: Exceptionally Well-Preserved Animals from 530 Million Years Ago: Kunming, Yunnan Science and Technology Press, 170 p. [in Chinese]
Hou, X.G., Aldridge, R.J., Bergström, J., Siveter, David J., Siveter, Derek J., and Feng, X.H., 2004, The Cambrian fossils of Chengjiang, China: the flowering of early animal life: Oxford, Blackwell, 248 p.
Hou, X.G., David, J.S., Derek, J.S., Richard, J.A., Cong, P.Y., Sarah, E.G., Ma, X.Y., Mark, A.P., and Mark, W., 2017, The Cambrian fossils of Chengjiang, China: the flowering of early animal life: Hoboken, New Jersey, John Wiley and Sons Publishing, 316 p.
Hu, S.X., 2005, Taphonomy and Palaeoecology of the Early Cambrian Chengjiang Biota from eastern Yunnan, China: Palaeobiologische Abhandlungen, v. 7, p. 1–197.
Hu, S.X., Zhu, M.Y., Luo, H.L., Steiner, M., and Zhao, F.C., 2013, The Guanshan Biota: Kunming, Yunnan Science and Technology Press, 204 p. [in Chinese]
Jago, J.B., Zang, W.L., Sun, X., Brock, G.A., Paterson, J.R., and Skovsted, C.B., 2006, A review of the Cambrian biostratigraphy of South Australia: Palaeoworld, v. 15, p. 406–423.
Jago, J.B., Gehling, J.G., Paterson, J.R., Brock, G.A., and Zang, W.L., 2012, Cambrian stratigraphy and biostratigraphy of the Flinders Ranges and the north coast of Kangaroo Island, South Australia: Episodes, v. 35, p. 247–255.
Jin, Y.G., Hou, X.G., and Wang, H.Y., 1993, Lower Cambrian pediculate lingulids from Yunnan, China: Journal of Paleontology, v. 67, p. 788–798.
Koneva, S.P., 1979, Stenothecoids and Inarticulate Brachiopods from the Lower and Lower Middle Cambrian of Central Kazakhstan: Alma-Ata, Nauka, 123 p. [in Russian]
Koneva, S.P., and Popov, L.E., 1983, On some new lingulids from the upper Cambrian and Lower Ordovician of Malyi Karatau Range, *in* Apollonov, M.K., Bandaletov, S.M., and Ivshin, N.K., eds., Stratigrafiya i paleontologiya nizhnego paleozoya Kazakhstana: Alma-Ata, Nauka, p. 112–124. [in Russian]
Kuhn, O., 1949, Lehrbuch der Paläozoologie: Stuttgart, Schweizerbart, 326 p.
Li, G.X., and Holmer, L.E., 2004, Early Cambrian lingulate brachiopods from the Shaanxi Province, China: GFF, v. 126, p. 193–211.
Li, G.X., Zhang, Z.F., Rong, J.Y., and Liu, D.Y., 2017, Cambrian brachiopod genera on type species of China, *in* Rong, J.Y., Jin, Y.G., Shen, S.Z., and Zhan, R.B., eds. Phanerozoic Brachiopod Genera of China: Beijing: Science Press, p. 39–85.
Liang, Y., Holmer, L.E., Skovsted, C.B., Duan, X.L., and Zhang, Z.F., 2020, Shell structure, ornamentation and affinity of the problematic early Cambrian brachiopod *Heliomedusa orienta*: Lethaia, v. 53, p. 574–587. https://doi.org/10.1111/let.12379.
Lin, T.R., Peng, S.C., and Zhu, X.J., 2004. Restudy on the Eodiscoids from the Shuijingtuo Formation (early Cambrian) in eastern Yangtze Gorge area, western Hubei: Acta Palaeontologica Sinica, v. 43, p. 502–514. [in Chinese with English summary]
Liu, F., Chen, F.Y., Chen, Y.L., and Zhang, Z.F., 2017, Note on the Shipai Biota (Cambrian Series 2, Stage 4) yielded from a new section (Xiachahzuang) in the Maoping Town of Zigui County, western Hubei Province, South China: Acta Palaeontologica Sinica, v. 55, p. 403–423. [in Chinese with English summary]

Liu, F., Skovsted, C.B., Topper, T.P., Zhang, Z.F., and Shu, D.G., 2020, Are hyoliths Palaeozoic lophophorates: National Science Review, v. 7, p. 453–469.
Liu, J.N., Ou, Q., Han, J., Zhang, Z.F., He, T.J., Yao, X.Y., Fu, D.J., and Shu, D.G., 2012. New occurrence of the Cambrian (Stage 4, Series 2) Guanshan Biota in Huize, Yunnan, South China: Bulletin of Geosciences, v. 87, p. 125–132.
Liu, Y.J., Zhao, Y.L., Liu, Y.Y., and Mao, Y.Q, 2015, A preliminary study of *Kutorgina* Billings, 1861 from the Cambrian 'Tsingsutung Formation' of Guizhou, China: Acta Palaeontologica Sinica, v. 54, p. 342–350. [in Chinese with English summary]
Lu, Y.H., 1979, Sedimentary Mineral of the Cambrian from China and Biology-Environment Cybernetics: Beijing, Geology Publishing House, 75 p. [in Chinese]
Luo, H.L., Li, Y., Hu, S.X., Fu, X.P., Hou, S.G., Liu, X.Y., Chen, L.Z., Li, F.J., Pang, J.Y., and Liu, Q., 2008, Early Cambrian Malong Fauna and Guanshan Fauna from Eastern Yunnan, China: Kunming, Yunnan Science and Technology Press, 134 p. [in Chinese]
Malakhovskaya, Y.E., 2013, Morphogenesis and evolution of *Kutorgina* Billings, 1861 (Brachiopoda, Kutorginida): Paleontological Journal, v. 47, p. 11–22.
Matthew, G.F., 1902. Notes on Cambrian faunas: Royal Society of Canada Transactions (Ser. 2, Sect. 4), v. 8, p. 93–112.
Menke, C.T., 1828, Synopsis methodica Molluscorum generum omnium et specierum earum, quae in Museo Menkeano adservantur; cum synonymia critica et novarum speicerum diagnosibus: Pyrmonti, Henrici Gelpke, 91p.
Mergl, M., 2019, Lingulate brachiopods of Tremadocian age from the abandoned Gabriela mine (Krušná Hora, central bohemia, Czech Republic): Folia Palaeobiologica, v. 52, p. 7–19.
Mergl, M., and Kordule, V., 2008, New middle Cambrian lingulate brachiopods from the Skryje-Tyrovice area (central Bohemia, Czech Republic): Bulletin of Geosciences, v. 83, p. 11–22.
Pan, B., Skovsted, C.B., Brock, G.A., Topper, T.P., Holmer, L.E., Li, L.Y., and Li, G.X., 2019, Early Cambrian organophosphatic brachiopods from the Xinji Formation, at Shuiyu section, Shanxi Province, North China: Palaeoworld, v. 29, p. 512–533. https://doi.org/10.1016/j.palwor.2019.07.001.
Pelman, Y.L., 1977, Ranne-i Srednekembriiskije bezzamkovye brakhiopody Sibirskoi platformy: Trudy Instituta Geologii i Geofiziki Akademiya Nauk SSSR, Sibirskoe Otdelenie, v. 316, p. 1–168. [in Russian]
Popov, L.E., and Tikhonov, U.A., 1990, Early Cambrian brachiopods from southern Kirgizia: Paleontologicheskii Zhurnal, v. 3, p. 33–46. [in Russian]
Popov, L.E., and Ushatinskaya, G.T., 1986, On secondary changes in the microstructure of calcium-phosphatic shells of inarticulate brachiopods, Izvestiya Akademii Nauk SSSR, Seriya Geologicheskaya, v. 10, p. 135–137. [in Russian]
Popov, L.E., Holmer, L.E., Rowell, A.J., and Peel, J.S., 1997, Early Cambrian brachiopods from North Greenland: Palaeontology, v. 40, p. 337–354.
Popov, L.E., Holmer, L.E., Hughes, N.C., Ghobadi Pour, M., and Myrow, P.M., 2015, Himalayan Cambrian brachiopods: Papers in Palaeontology, v. 1, p. 345–399.
Poulsen, V., 1932, The lower Cambrian faunas of East Greenland: Meddelelser om Grønland, v. 87, 66 p.
Poulsen, V., 1971, Notes on an Ordovician acrotretacean brachiopod from the Oslo region: Bulletin of the Geological Society of Denmark, v. 20, p. 265–278.
Roberts J., and Jell P.A., 1990, Early middle Cambrian (Ordian) brachiopods of the Coonigan Formation, western New South Wales: Alcheringa, v. 14, p. 257–309.
Rohlf, F.J., 2015, The tps series of software: Hystrix, the Italian Journal of Mammalogy, v. 26, p. 1–4.
Rong, J.Y., 1974, Cambrian brachiopods, *in* Nanjing Institute of Geology, ed., Handbook of Palaeontology and Stratigraphy of Southwest China: Beijing, Science Press, p. 113–114.
Rowell, A.J., 1986, The distribution and inferred larval dispersion of *Rhondellina dorei*: a new Cambrian brachiopod (Acrotretida): Journal of Paleontology, v. 60, p. 1056–1065.
Rowell, A.J., and Caruso, N.E., 1985, The evolutionary significance of *Nisusia sulcata*, an early articulate brachiopod: Journal of Paleontology, v. 59, p. 1227–1242.
Schuchert, C., 1893, A classification of the Brachiopoda: American Geologist, v. 11, p. 141–167.
Sepkoski, J.J., Bambach, R.K., Raup, D.M., and Valentine, J.W., 1981, Phanerozoic marine diversity and the fossil record: Nature, v. 293, p. 435–437.
Skovsted, C.B., and Holmer, L.E., 2003, The Early Cambrian stem group brachiopod *Mickwitzia* from Northeast Greenland: Acta Palaeontologica Polonica, v. 48, p. 11–30.
Skovsted, C.B., and Holmer, L.E., 2005, Early Cambrian brachiopods from North-East Greenland: Palaeontology, v. 48, p. 325–345.
Skovsted, C.B., and Holmer, L.E., 2006, The lower Cambrian brachiopod *Kyrshabaktella* and associated shelly fossils from the Harkless Formation, southern Nevada: GFF, v. 128, p. 327–337.
Skovsted, C.B., Clausen, S., Álvaro, J.J., and Ponlevé, D.P., 2014, Tommotiids from the early Cambrian (Series 2, Stage 3) of Morocco and the evolution of the tannuolinid scleritome and setigerous shell structures in stem group brachiopods: Palaeontology, v. 57, p. 171–192.
Smith, P.M., Brock, G.A., and Paterson, J.R., 2015, Fauna and biostratigraphy of the Cambrian (Series 2, Stage 4; Ordian) Tempe Formation (Pertaoorrta Group), Amadeus Basin, Northern Territory: Alcheringa: An Australasian Journal of Palaeontology, v. 39, p. 40–70.
Steiner, M., Li, G.X., Qian, Y., Zhu, M.Y., and Erdtmann, B.D., 2007, Neoproterozoic to early Cambrian small shelly fossil assemblages and a revised biostratigraphic correlation of the Yangtze Platform (China): Palaeogeography, Palaeoclimatology, Palaeoecology, v. 254, p. 67–99.
Steiner, M., Yang, B., Hohl, S., Zhang, L., Chang, S., 2020, Cambrian small skeletal fossil and carbon isotope records of the southern Huangling Anticline, Hubei (China) and implications for chemostratigraphy of the Yangtze Platform: Palaeogeography, Palaeoclimatology, Palaeoecology, v. 554, 109817. https://doi.org/10.1016/j.palaeo.2020.109817.
Streng, M., 1999, Early middle Cambrian representatives of the superfamily Acrotretoidea (Brachiopoda) from Morocco: Zeitschrift der Deutschen Geologischen Gesellschaft, v. 150, p. 27–87.
Streng, M., and Holmer, L.E., 2006, New and poorly known acrotretid brachiopods (Class Lingulata) from the *Cedaria-Crepicephalus* zone (late middle Cambrian) of the Great Basin, USA: Geobios, v. 39, p. 125–154.
Streng, M., Holmer, L.E., Popov, L.E., and Budd, G.E., 2008, Columnar shell structures in early linguloid brachiopods—new data from the middle Cambrian of Sweden: Earth and Environmental Science Transactions of the Royal Society of Edinburgh, v. 98, p. 221–232.
Sun, W.G., and Hou, X.G., 1987, Early Cambrian medusae from Chengjiang, Yunnan, China: Acta Palaeontologica Sinica, v. 26, p. 257–270. [in Chinese with English summary]
Topper, T.P., Guo, J.F., Clausen, S., Skovsted, C.B., and Zhang, Z.F., 2019, A stem group echinoderm from the basal Cambrian of China and the origins of Ambulacraria: doi: /10.1038/s41467-019-09059-3.
Ushatinskaya, G.T., 2016, Protegulum and brephic shell of the earliest organophosphatic brachiopods: Paleontological Journal, v. 50, p. 141–152.
Ushatinskaya, G.T., and Korovnikov, I.V., 2019, Revision of the early and middle Cambrian acrotretids (Brachiopoda, Linguliformea) from the Siberian Platform: Paleontological Journal, v. 53, p. 689–714.
Ushatinskaya, G.T., and Malakhovskaya, Y.E., 2001, Origin and development of the Cambrian brachiopod biochores: Stratigraphy and Geological Correlation, v. 9, p. 540–556.
Ushatinskaya, G.T., Zezina, O.N., Popov, L.E., and Putivtseva, N.V., 1988, On the microstructure and composition of brachiopods with calcium phosphate shell: Paleontoligicheskii Zhurnal, v. 1, p. 45–55. [in Russian]
Voronova, L.G., Drozdova, N.A., Esakova, N.V., Zhegallo, E.A., Zhuravlev, A.Y., Rozanov, A.Y., and Ushatinskaya, G.T., 1987, Lower Cambrian fossils of the Mackenzie Mountains (Canada): Trudy Instituta Geologii i Geofiziki, Akademiya Nauk SSSR, Sibirskoe Otdelenie, v. 224, p. 1–88.
Waagen, W., 1885, Salt Range fossils, *Productus*-Limestone fossils, Brachiopoda: Palaeontologia Indica, v. 13, p. 729–770.
Walcott C D., 1885, Paleontologic notes: American Journal of Science, v. 29, p. 114–117.
Walcott, C.D., 1905, Cambrian Brachiopoda with descriptions of new genera and species: Proceedings of the United States National Museum, v. 18, p. 227–337.
Walcott, C.D., 1908, Cambrian Brachiopoda: descriptions of new genera and species. Smithsonian Miscellaneous Collections, v. 53, p. 53–137.
Wang, H.Z., Zhang, Z.F., Holmer, L.E., Hu, S.X., Wang, X.R., and Li, G.X., 2012, Peduncular attached secondary tiering acrotretoid brachiopods from the Chengjiang fauna: implications for the ecological expansion of brachiopods during the Cambrian explosion: Palaeogeography, Palaeoclimatology, Palaeoecology, v. 323, p. 60–67.
Wang, X.F., Ni, S.Z., Zeng, Q.L., Xu, G.H., Zhou, T.M., Li, Z.H., and Lai, C.G., 1987, Biostratigraphy of the Yangtze Gorge Area, Part, 2. Early Palaeozoic Era: Beijing, Geological Publishing House, 640 p. [in Chinese]
Wang, X.F., Stouge, S., Chen, X.H., C., Li, Z.H., Wang, C.S., Finney, S.C., Zeng., Q.L., Zhou, Z.Q., Chen, H.M., and Erdtmann, B.D., 2009, The Global Stratotype Section and Point for the base of the Middle Ordovician Series and the Third Stage (Dapingian): Episodes, v. 32, p. 96–113.
Williams, A., and Holmer, L.E., 1992, Ornamentation and shell structure of acrotretoid brachiopods: Palaeontology, v. 35, p. 657–692.
Williams, A., and Holmer, L.E., 2002, Shell structure and inferred growth, functions and affinities of the sclerites of the problematic *Micrina*: Palaeonotology, v. 45, p. 845–873.

Williams, A., Carlson, S.J., Brunton, C., Holmer, L.E., and Popov, L.E., 1996. A supra-ordinal classification of the Brachiopoda: Philosophical Transactions of the Royal Society of London, Series B, v. 351, p. 1171–1193.
Williams, A., Brunton, C.H.C., and Carlson, S.J., eds., 1997, Treatise on Invertebrate Paleontology, Part H, Brachiopoda (Revised): Boulder, Colorado and Lawrence, Kansas, Geological Society of America and University of University of Kansas Press, 3226 p.
Williams, A., James, M.A., Emig, C.C., Mackay, S., and Rhodes, M.C., 2000, Anatomy, *in* Kaesler, R.L., ed, Treatise on Invertebrate Paleontology, Part H 1, Brachiopoda: Boulder, Colorado and Lawrence, Kansas, Geological Society of America and University of Kansas Press, p. H7–H188.
Yang, B., Steiner, M., and Keupp, H., 2015, Early Cambrian palaeobiogeography of the Zhenba Fangxian Block (South China): independent terrane or part of the Yangtze Platform?: Gondwana Research, v. 28, p. 1543–1565.
Yang, Y.N., and Zhang, X.L., 2016, The Cambrian palaeoscolecid *Wronascolex* from the Shipai fauna (Cambrian Series 2, Stage 4) of the Three Gorges area, South China: Papers in Palaeontology, v. 2, p. 555–568.
Zeng, Q.L., 1987, Brachiopoda, *in* Wang, X.F., ed., Biostratigraphy of the Yangtze Gorge Area, Part 2. Early Palaeozoic Era: Beijing, Geological Publishing House, p. 209–245. [in Chinese]
Zhang, W.T., Lu, Y.H., Zhu, Z.L., Qian, Y., Lin, H.Z., Zhou, Z.Y., Zhang, S.G., and Yuan, J.L., 1980, Cambrian trilobite faunas of Southwest China: Beijing: Science Press, 497 p. [in Chinese]
Zhang, X.L., and Hua, H., 2005, Soft-bodied fossils from the Shipai Formation, lower Cambrian of the Three Gorge area, South China: Geological Magazine, v. 142, p. 699–709.
Zhang, X.L., and Shu, D.G., 2014, Causes and consequences of the Cambrian explosion: Chinese Science Earth Science, v. 57, p. 930–942.
Zhang, X.L., Liu, W., and Zhao, Y., 2008, Cambrian Burgess Shale-type Lagerstätten in South China: distribution and significance: Gondwana Research, v. 14, p. 255–262.
Zhang, Z.F., and Han, J., 2004, A new linguliform brachiopod from the Chengjiang Lagerstätte: Journal of Northwest University, v. 34, p. 450–452. [in Chinese with English summary]
Zhang, Z.F., and Holmer, L.E., 2013, Exceptionally preserved brachiopods from the Chengjiang Lagerstätte (Yunnan, China): perspectives on the Cambrian explosion of metazoans: National Science in China, v. 21, p. 66–80.
Zhang, Z.F., Han, J., Zhang, X.L., Liu, J.N., and Shu, D.G., 2003, Pediculate brachiopod *Diandongia pista* from the lower Cambrian of South China: Acta Geologica Sinica (English Edition), v. 77, p. 288–293.
Zhang, Z.F., Shu, D.G., Han, J., and Liu, J.N., 2004, New data on the lophophore anatomy of Early Cambrian linguloids from the Chengjiang Lagerstätte, Southwest China: Carnets de Géologie/Notebooks on Geology, Cg2004. https://doi.org/10.4267/2042/310.
Zhang, Z.F., Shu, D.G., Han, J., and Liu, J.N., 2005, Morpho-anatomical differences of the early Cambrian Chengjiang and recent lingulids and their implications: Acta Zoologica, v. 86, p. 277–288.
Zhang, Z.F., Han, J., Zhang, X.L., Liu, J.N., Guo, J.F., and Shu, D.G., 2007a, Note on the gut preserved in the lower Cambrian *Lingulellotreta* (Lingulata, Brachiopoda) from southern China: Acta Zoologica, v. 88, p. 65–70.
Zhang, Z.F., Shu, D.G., Emig, C., Zhang, X.L., Han, J., Liu, J.N., and Guo, J.F., 2007b, Rhynchonelliformean brachiopods with soft-tissue preservation from the early Cambrian Chengjiang Lagerstätte of South China: Palaeontology, v. 50, p. 1391–1402.
Zhang, Z.F., Robson, S.P., Emig, C., and Shu, D.G., 2008, Early Cambrian radiation of brachiopods: A perspective from South China: Gondwana Research, v. 14, p. 241–254.
Zhang, Z.F., Li, G.X., Holmer, L.E., Brock, G.A., Balthasar, U., Skovsted, C.B., Fu, D.J., Zhang X.L., Wang, H.Z., Butler, A., Zhang Z.L., Cao, C.Q., Han, J., Liu, J.N., and Shu, D.G., 2014, An early Cambrian agglutinated tubular lophophorate with brachiopod characters: Scientific Reports, v. 4, 4682. https://doi.org/10.1038/srep04682.
Zhang, Z.F., Zhang, Z.L., Holmer, L.E., and Li, G.X., 2015, First report of linguloid brachiopods with soft parts from the lower Cambrian (Series 2, Stage 4) of the Three Gorges area, South China: Annales de Paléontologie, v. 101, p. 167–177.
Zhang, Z.F., Zhang, Z.L., Li, G.X., and Holmer, L.E., 2016, The Cambrian brachiopod fauna from the first-trilobite age Shuijingtuo Formation in the Three Gorges area of China: Palaeoworld, v. 25, p. 333–355.
Zhang, Z.F., Holmer, L.E., Liang, Y., Chen, Y.L., and Duan, X.L., 2020a, The oldest '*Lingulellotreta*' (Lingulata, Brachiopoda) from China and its phylogenetic significance: integrating new material from the Cambrian Stage 3–4 Lagerstätten in eastern Yunnan, South China: Journal of Systematic Palaeontology, v. 18, p. 1–29. https://doi.org/10.1080/14772019.2019.1698669.
Zhang, Z.F., Strotz, L.C., Topper, T.P., Chen, F.Y., Chen, Y.L., Liang, Y., Zhang, Z.L., Skovsted, C.B., and Brock, G.A., 2020b, An encrusting kleptoparasite-host interaction from the early Cambrian: Nature Communications, v. 11, 2625. https://doi.org/10.1038/s41467-020-16332-3.
Zhang, Z.L., Zhang, Z.F., and Wang, H.Z., 2016, Epithelial cell moulds preserved in the earliest acrotretid brachiopods from the Cambrian (Series 2) of the Three Gorges area, China: GFF, v. 138, p. 455–466.
Zhang, Z.L., Popov, L.E., Holmer, L.E., and Zhang, Z.F., 2018a, Earliest ontogeny of early Cambrian acrotretoid brachiopods first evidence for metamorphosis and its implications: BMC evolutionary biology, v. 18, p. 42.
Zhang, Z.L., Zhang, Z.F., Holmer, L.E., and Chen, F.Y., 2018b, Post-metamorphic allometry in the earliest acrotretoid brachiopods from the lower Cambrian (Series 2) of South China, and its implications: Palaeontology, v. 61, p. 183–207.
Zhang, Z.L., Chen, F.Y., and Zhang, Z.F., 2020, Earliest phosphatic-shelled brachiopods from the carbonates of South China—their diversification, ontogeny, and distribution: Earth Science Frontiers, v. 27, p. 79–103. https://doi.org/10.13745/j.esf.sf.2020.6.4. [in Chinese with English summary]
Zhu, M.Y., Zhang, J.M., and Yang, A.H., 2007, Integrated Ediacaran (Sinian) chronostratigraphy of South China: Palaeogeography Palaeoclimatology Palaeoecology, v. 254, p. 7–61.
Zhu, M.Y., Yang, A.H., Yuan, J.L., Li, G.X., Zhang, J.M., Zhao, F.C., Ahn, S.Y., and Miao, L.Y., 2019, Cambrian integrative stratigraphy and timescale of China: Science China Earth Sciences, v. 62, p. 25–60.

Accepted: 21 December 2020